

## **Response to Interactive comment on “A multi-scale comparison of modeled and observed seasonal methane cycles in northern wetlands”**

We would like to thank the editor and the two anonymous reviewers for carefully reviewing this manuscript and providing constructive suggestions that significantly strengthen this study. The following document (in blue) details the authors' responses to reviewers' comments followed by the new draft of manuscript with highlighted revisions (in yellow).

### **Response to Referee #1:**

#### **Anonymous Referee #1**

Received and published: 4 July 2016

The paper is devoted to calibration and validation of the CLM4Me model, that is the methane module embedded in the Community Land Model, version 4.5. It presents an important step towards further model development, i.e. the identification of the major drawbacks of the model performance in the area of northern wetlands. The methane model output is compared to different sources of data, covering spatial scales from particular sites (towers, chambers), through regional (WRF-based footprint analysis) to global (inverse modeling estimates). The parameter, characterizing the aerenchyma area, was tuned to get better agreement with empirical data on surface CH<sub>4</sub> emissions. Two methods of inundation parameterization were applied, and compared in the model output. The special focus is made on the Alaskan methane emissions, however a number of chamber and eddy covariance measurements from Swedish and Finnish sites are involved in the model validation as well. One of the main results of the study is that CLM4Me significantly underestimates wintertime CH<sub>4</sub> fluxes calling for deeper understanding of snow-period methane release to the atmosphere from terrestrial ecosystems.

I don't have principal concerns on the results of this study. There are some suggestions, however, which I hope could improve the paper:

- The title of the paper presumes a wider scope that has been actually taken place in the study: "cycles" mean much more than "emissions". I suggest to change the title as: "A multiscale comparison of modeled and observed seasonal methane emissions in northern wetlands"

*Authors:* We replaced “cycles” by “emissions”.

- The structure of the paper could be bettered. For instance, in the model description section 2.1.1 some of the model results are discussed. I recommend to move the latter to the appropriate sections.

*Authors:* We moved the results from section 2.1.1 to section 3.1.

- I could not understand why aerenchyma-related parameter S was the only one that was calibrated, whereas there are lot of others in any methane model. Moreover, I didn't see any significant impact of changing S on the zonally-averaged methane emission annual cycle in the northern latitudes, depicted at Fig.1, whereas such an impact had been anticipated as one of the main points of the paper.

*Authors:* In this study, we did not intend to make a full parametric uncertainty quantification, but rather to fix the issue that was responsible for the unrealistic CH<sub>4</sub> emission seasonal pattern (very high CH<sub>4</sub> emissions in the thaw period followed by relatively low CH<sub>4</sub> emissions through the growing season in inundated areas). We only calibrated the aerenchyma-related parameter S because we found the original assumption related to aerenchyma area caused the unrealistic high latitude seasonal pattern of CH<sub>4</sub> emissions. We also performed sensitivity analyses of other parameters, including those for CH<sub>4</sub> production, oxidation, and transport pathways (e.g.,  $f_N$  in aerenchyma transport) and found that other parameters have minimum impact on the unrealistic seasonal pattern. To clarify these points, we added to section 3.1 the sentence “We performed sensitivity analyses of all the parameters affecting seasonal CH<sub>4</sub> production, oxidation, and emission pathways and found that the parameterization of aerenchyma transport had the greatest impact on the seasonal CH<sub>4</sub> emissions in saturated areas.” Compared with CarbonTracker predictions, our changes resulted in several CLM CH<sub>4</sub> emission prediction biases being reduced (e.g., overestimation between 30 and 60 °N in May and June, underestimated growing-season CH<sub>4</sub> emissions north of 56°N, and overestimated CH<sub>4</sub> emissions in 2-53°N and 34-56°S; Fig. 1d and f).

- I have a number of more specific remarks, that are given as **sticky notes** in the manuscript pdf. I propose to accept the paper for publication after corresponding revision.

*Authors:* All the responses and revisions to sticky notes are incorporated into the new drafts (attached) of this manuscript.

## Response to Referee #2:

### Anonymous Referee #2

Received and published: 5 July 2016

General Comments: I liked to read this paper as they used an improved CLM-BGC model to estimate the methane fluxes from northern wetland and compared the model- estimated methane fluxes with static chamber measurements, eddy covariance and aircraft measurements. However, I see some major shortcomes which need to be addressed in a revision. Specific comments:

- 1. In this study, the major improvement of the CLM4.5-BGC is related to the methane transport through aerenchyma. In the Equation 2 (Line 210), several parameters were used to calculate the aerenchyma area. However, the author only analyzed

and discussed the variation of “S”. Why? I missed to see the discussion at this point. How about fN (belowground fraction of current NPP)? Is this a fixed parameter or it will change during different growing stages? If it is a fixed parameter, you should also discuss the related uncertainties.

*Authors:* We addressed this same point above in our response to Reviewer #1.

- 2. In the Section 3.1 (Line 350-362), the author compared the model-estimated results with TD and BU estimation from Kirschke et al., 2013, which was unexpected. It seems that the whole manuscript was talking about the methane fluxes from northern high latitude (mostly in Alaska). And the wetland types in the tropical regions are very different from the ones in high latitude region. I suggested to remove this part or only focus on the northern wetland, and make the whole manuscript more consistent.

*Authors:* Since CLM is a global model, changes to a parameter will have effects globally. We compared the results with TD and BU estimation from Kirschke et al., 2013 to clarify that the improved model predictions extended globally.

- 3. In the Section 3.2.1, there should be further discussion about the overestimation, underestimation and misrepresentation of seasonal emission from CLM compared with site-level observation, especially for Figure 2a, b, d, h and k. Otherwise, it was hard to say CLM has the capability to reproduce the methane fluxes.

*Authors:* A detailed site-level comparison was not a goal of this paper, since the model was not initialized at each site, nor were parameters chosen specifically for sites. Instead, we describe in the text the potential reasons for the misrepresentation of seasonal emissions from CLM, and note that the reasons vary by site and year.

- 4. It is good to make the unit consistent throughout the manuscript, especially in Section 3.2.2. It made readers very confusing to have different units even within the same paragraph.

*Authors:* We revised to use the same unit of CH<sub>4</sub> emissions (mg CH<sub>4</sub> m<sup>-2</sup> day<sup>-1</sup>). Accordingly, we updated Fig.1 to use the same unit.

- 5. In Section 3.3, I was just curious about the analysis of temperature and precipitation. Did the author analyze the temperature and precipitation over Northern wetland (only inundated area)? Line 525-527, it is hard to read the bias from the Fig. 6.

*Authors:* The temperature and precipitation anomalies are calculated over all of Alaska. In Fig. 6, the modeled wintertime CH<sub>4</sub> emissions (blue and green lines) are much smaller than the CarbonTracker CH<sub>4</sub> emissions (brown line).

1 **A multi-scale comparison of modeled and observed seasonal methane**  
2 **emissions in northern wetlands**

3  
4 Xiyan Xu<sup>1</sup>, William J. Riley<sup>1</sup>, Charles D. Koven<sup>1</sup>, Dave P. Billesbach<sup>2</sup>, Rachel Y.-W.  
5 Chang<sup>3, 4</sup>, Róisín Commane<sup>3</sup>, Eugénie S. Euskirchen<sup>5</sup>, Sean Hartery<sup>4</sup>, Yoshinobu  
6 Harazono<sup>6, 7</sup>, Hiroki Iwata<sup>6, 8</sup>, Kyle C. McDonald<sup>9, 10</sup>, Charles E. Miller<sup>10</sup>, Walter C.  
7 Oechel<sup>11, 12</sup>, Benjamin Poulter<sup>13</sup>, Naama Raz-Yaseef<sup>1</sup>, Colm Sweeney<sup>14, 15</sup>, Margaret  
8 Torn<sup>1, 16</sup>, Steven C. Wofsy<sup>3</sup>, Zhen Zhang<sup>15, 17</sup>, Donatella Zona<sup>11, 18</sup>

9  
10 <sup>1</sup>Earth Sciences Division, Lawrence Berkeley National Laboratory, Berkeley, California,  
11 USA;

12 <sup>2</sup>Biological System Engineering Department, University of Nebraska, Lincoln,  
13 Nebraska;

14 <sup>3</sup>School of Engineering and Applied Sciences, Harvard University, Cambridge,  
15 Massachusetts, USA;

16 <sup>4</sup>Department of Physics and Atmospheric Science, Dalhousie University, Halifax,  
17 Nova Scotia, Canada;

18 <sup>5</sup>Institute of Arctic Biology, University of Alaska Fairbanks, Fairbanks, Alaska, USA;

19 <sup>6</sup>International Arctic Research Center, University of Alaska Fairbanks, Fairbanks, Alaska,  
20 USA;

21 <sup>7</sup>Graduate School of Life and Environmental Sciences, Osaka Prefecture University,  
22 Sakai, Osaka, Japan;

23 <sup>8</sup>Department of Environmental Sciences, Faculty of Science, Shinshu University,  
24 Matsumoto, Nagano, Japan;

25 <sup>9</sup>Department of Earth and Atmospheric Sciences, CUNY Environmental Crossroads  
26 Initiative and NOAA-CREST Institute, The City College of New York, City University  
27 of New York, New York

28 <sup>10</sup>Jet Propulsion Laboratory, California Institute of Technology, Pasadena, California,  
29 USA;

30 <sup>11</sup>Global Change Research Group, Department of Biology, San Diego State University,  
31 San Diego, California, USA;

32 <sup>12</sup>Department of Environment, Earth and Ecosystems, The Open University, Milton  
33 Keynes, U. K. MK7 6AA;

34 <sup>13</sup>Department of Ecology, Montana State University, Bozeman, MT 59717, USA

35 <sup>14</sup>Cooperative Institute for Research in Environmental Sciences, University of Colorado,  
36 Boulder, CO, 80304

37 <sup>15</sup>NOAA Earth System Research Laboratory, Global Monitoring Division, Boulder, CO,  
38 USA

39 <sup>16</sup>Energy and Resources Group, University of California-Berkeley, Berkeley,  
40 California, USA;

41 <sup>17</sup>Swiss Federal Research Institute WSL, Birmensdorf 8059, Switzerland

42 <sup>18</sup>Department of Animal and Plant Sciences, University of Sheffield, Sheffield  
43 S102TN, United Kingdom.

44

45 Correspondence to : Xiyan Xu (xxu@lbl.gov)

46

47 **Abstract:**

48 Wetlands are the largest global natural methane (CH<sub>4</sub>) source, and emissions between  
49 50°N and 70°N latitude contribute 10-30% to this source. Predictive capability of land  
50 models for northern wetland CH<sub>4</sub> emissions is still low due to limited site measurements,  
51 strong spatial and temporal variability in emissions, and complex hydrological and  
52 biogeochemical dynamics. To explore this issue, we compare wetland CH<sub>4</sub> emission  
53 predictions from the Community Land Model 4.5 (CLM4.5-BGC) with site to regional  
54 scale observations. A comparison of the CH<sub>4</sub> fluxes with eddy flux data highlighted  
55 needed changes to the model's estimate of aerenchyma area, which we implemented and  
56 tested. The model modification substantially reduced biases in CH<sub>4</sub> emissions when  
57 compared with CarbonTracker CH<sub>4</sub> predictions. CLM4.5 CH<sub>4</sub> emission predictions agree  
58 well with growing season (May-September) CarbonTracker Alaskan regional-level CH<sub>4</sub>  
59 predictions and site-level observations. However, CLM4.5 underestimated CH<sub>4</sub> emissions  
60 in the cold season (October-April). The monthly atmospheric CH<sub>4</sub> mole fraction  
61 enhancements due to wetland emissions are also assessed using the WRF-STILT  
62 Lagrangian transport model coupled with daily emissions from CLM4.5 and compared  
63 with aircraft CH<sub>4</sub> mole fraction measurements from the Carbon in Arctic Reservoirs  
64 Vulnerability Experiment (CARVE) campaign. Both the tower and aircraft analyses  
65 confirm the underestimate of cold season CH<sub>4</sub> emissions by CLM4.5. The greatest  
66 uncertainties in predicting the seasonal CH<sub>4</sub> cycle are from the wetland extent, cold  
67 season CH<sub>4</sub> production and CH<sub>4</sub> transport processes. We recommend more cold-season  
68 experimental studies in high latitude systems, which could improve understanding and  
69 parameterization of ecosystem structure and function during this period. Predicted CH<sub>4</sub>  
70 emissions remain uncertain, but we show here that benchmarking against observations  
71 across spatial scales can inform model structural and parameter improvements.

72

## 73 1 Introduction

74 Natural wetlands are the largest natural methane (CH<sub>4</sub>) source, contributing up to  
75 34% of global CH<sub>4</sub> emissions (Kirschke et al., 2013). Between 1980 and 2009, estimated  
76 global annual CH<sub>4</sub> emissions from wetlands varied from 115 to 231 Tg CH<sub>4</sub> in top-down  
77 atmospheric inversion models and 169 to 284 Tg CH<sub>4</sub> in bottom-up process-based land  
78 models (Kirschke et al., 2013). Peat-rich bogs and fens lying between 50°N and 70°N  
79 constitute about half of the global wetland area, and release 10-30% of the total wetland  
80 CH<sub>4</sub> (Wania et al., 2010; Zhuang et al., 2004; Bergamaschi et al., 2009; Riley et al.,  
81 2011). Much of the northern wetland area is in the permafrost zone, which stores  
82 1035±150 Pg soil organic carbon for the 0-3m soil depth (Hugelius et al., 2014). When  
83 permafrost soils thaw, CH<sub>4</sub> is produced under anaerobic conditions by methanogenic  
84 archaea. Once CH<sub>4</sub> is produced, it can be oxidized by methanotrophic archaea. CH<sub>4</sub>  
85 surface emissions occur through several transport pathways: aqueous and gaseous  
86 diffusion, ebullition, and aerenchyma diffusion and advection. At any point in the soil,  
87 the CH<sub>4</sub> concentration is governed by the balance between CH<sub>4</sub> production in anoxic  
88 zones, CH<sub>4</sub> consumption in oxic zones, transport, and atmospheric CH<sub>4</sub> diffusion at the  
89 soil-atmosphere interface.

90 Many interacting factors (e.g., temperature, thaw depth, soil moisture, depth of the  
91 water table, vegetation type) affect CH<sub>4</sub> production and emission. CH<sub>4</sub> production has a  
92 positive response to temperature increase (Van Hulzen et al., 1999; van Winden et al.,  
93 2012; Hommeltenberg et al., 2014) and laboratory incubations of soil samples from the  
94 active layer show that large variability of Q<sub>10</sub> values for CH<sub>4</sub> production (1.5 to 28,  
95 Segers et al., 1998) is related to site-specific peatland type and organic matter quality  
96 (Lupascu et al., 2012). CH<sub>4</sub> emissions also show positive temperature dependence above  
97 freezing. The temperature dependence of surface CH<sub>4</sub> emission is much stronger than that  
98 of respiration and photosynthesis, which indicates increases in both CH<sub>4</sub> emissions and  
99 the ratio of CH<sub>4</sub> to CO<sub>2</sub> emissions with seasonal increases in temperature (Yvon-  
100 Durocher et al., 2014). The positive temperature dependence of CH<sub>4</sub> emissions may only  
101 be valid when CH<sub>4</sub> oxidation is less sensitive to temperature (van Winden et al., 2012).  
102 The Q<sub>10</sub> value for CH<sub>4</sub> oxidation was reported to be 1.4 to 2.1 in northern peat soils  
103 (Dunfield et al., 1993). Strong oxidation temperature sensitivity can lead to decreased  
104 CH<sub>4</sub> surface emissions with rising temperature (Wang et al., 2014). The positive  
105 dependence of CH<sub>4</sub> emissions on soil temperature can be most significant in areas with  
106 sufficient soil moisture or a shallow water table (Roulet et al., 1992; Moosavi et al., 1996;  
107 Wickland et al., 1999). The dependency of CH<sub>4</sub> emissions on temperature can vanish at  
108 high temperature and low water table (Hommeltenberg et al., 2014). At low water table  
109 levels, large CH<sub>4</sub> oxidation can mask the CH<sub>4</sub> production temperature sensitivity in the  
110 net emissions. CH<sub>4</sub> production under sub-zero temperatures was reported in incubation  
111 experiments (Clein and Schimel, 1995; Brouchkov et al., 2003), however, the  
112 mechanisms that regulate CH<sub>4</sub> production under cold temperatures have not been  
113 clarified.

114 Soil water content exerts strong control on CH<sub>4</sub> emissions by affecting  
115 belowground carbon decomposition and root growth (Iversen et al., 2015). A lowered  
116 water table typically reduces CH<sub>4</sub> production and emission, because of a higher aerobic to  
117 anaerobic respiration ratio in the soil column and CH<sub>4</sub> oxidation during diffusive



118 transport through the oxygen-rich surface layer (Whalen and Reeburgh, 1990). If CH<sub>4</sub>  
119 produced in anoxic zones (e.g., below the water table) is transported to the atmosphere  
120 through aerenchyma, the impact of methanotrophy on net CH<sub>4</sub> emissions is diminished  
121 (Bartlett et al., 1992; Torn and Chapin, 1993; King et al., 1998; Juutinen et al., 2003;  
122 McEwing et al., 2015). The reduced methanotrophic impacts vary with vascular species  
123 cover and root density and are more common in tall vegetation, because taller plants have  
124 more extensive root systems that enable more methanogenesis and pore water CH<sub>4</sub> to  
125 escape to the atmosphere (van Fischer et al., 2010). The correlation between water table  
126 depth and CH<sub>4</sub> emission can be very weak if the water table drops in an already oxic  
127 surface layer (Sturtevant et al., 2012).

128 The seasonal cycle of CH<sub>4</sub> emissions and their physical controls are strongly  
129 controlled by the freeze-thaw cycle in northern wetlands, and its regulation of wetland  
130 extent. The northern wetland area retrieved from the 19- and 37-GHz passive microwave  
131 Special Sensor Microwave/Image (SSM/I) brightness temperature database shows that  
132 maximum inundation is usually observed during July, August, and September in north  
133 America (48°N-68°N) and between June and September in northern Eurasia (Mialon et  
134 al., 2005). The inundation dynamics retrieved from SSM/I and ISCCP observations, ERS  
135 scatterometer responses, and AVHRR visible and near-infrared reflectance also show that  
136 maximum inundation occurs in July and August in northern boreal regions (55°N-70°N)  
137 (Prigent et al., 2007). The inferred wetland extent increases rapidly during the spring  
138 thaw period and shrinks again during the fall freeze period; though it is unclear at large  
139 scales how much of this seasonal cycle is due to changes in the areal fraction of land in  
140 which water ponds at the surface versus changes in the phase of that water. The  
141 interannual variability of high-latitude summer wetland extent is very small. Larger  
142 interannual variability during the intermediate seasons arises from the large variability of  
143 the timing and extent of snowmelt and accumulation (Mialon et al., 2005). For boreal  
144 bogs north to 50°N, the variation in wetland area contributed about 30% to the annual  
145 emissions and can explain the interannual variation in regional CH<sub>4</sub> emissions (Ringeval  
146 et al., 2010).

147 Site measurements have shown great variability in seasonal CH<sub>4</sub> emissions  
148 (Wilson et al., 1989; Mastepanov et al., 2008; 2013; Zona et al., 2016). In the late fall to  
149 winter, the surface water or shallow peat zone are frozen, and CH<sub>4</sub> produced below the  
150 frozen layer can be trapped. Only a small portion of the trapped CH<sub>4</sub> is oxidized because  
151 of low oxygen concentrations below the frozen layer (Mastepanov et al., 2008). Observed  
152 CH<sub>4</sub> emissions during spring thaw are highly variable and contribute substantially to total  
153 annual emissions. CH<sub>4</sub> fluxes during the spring thaw period contributed 11% to the  
154 annual budget over an aapa mire in Finnish Lapland (Hargreaves et al., 2001). The  
155 emission amounts can be 24% of the total annual emissions during the spring period after  
156 snowmelt next to an open pool in Caribou Bog, Maine, while the proportion can be as  
157 high as 77% in the adjacent upland area (Comas et al., 2008). In the non-inundated  
158 upland tundra, the cold season (September to May) emissions account for more than 50%  
159 of the annual CH<sub>4</sub> emissions (Zona et al., 2016). Although wetlands can contribute a large  
160 proportion of annual CH<sub>4</sub> emissions during the cold season, the seasonal peak of CH<sub>4</sub>  
161 emissions is usually observed in the summer (Pickett-Heaps et al., 2011; Zona et al.,  
162 2016). A transport model combined with flight measurements showed the peak CH<sub>4</sub>  
163 emission to be in July-August in the Hudson Bay Lowlands (Pickett-Heaps et al., 2011).

164 Although the recorded emission pulses during spring thaw and late fall (Song et al., 2012;  
165 Tokida et al., 2007; Rinne et al., 2007; Mastepanov et al., 2008; 2013) may be more  
166 localized and of minor importance to annual emissions (Chang et al., 2014; Rinne et al.,  
167 2007), the pulses indicates the complexity and heterogeneity in the seasonal CH<sub>4</sub> cycle.

168 Many modeling studies have shown that there is large uncertainty in predictions  
169 of spatial patterns of CH<sub>4</sub> emissions from natural wetlands at the regional and global  
170 scales (Melton et al., 2013; Bohn et al., 2015). This uncertainty can be roughly split into  
171 poor knowledge of water table and soil moisture dynamics versus poor knowledge of CH<sub>4</sub>  
172 fluxes per unit area of land with a given water table depth or soil moisture state; both  
173 contribute substantially to the overall uncertainty. One approach to reducing this overall  
174 uncertainty is to focus on the seasonal cycles of CH<sub>4</sub> emissions at the site scale (where  
175 inundation dynamics can be more easily constrained) versus at larger scales to ask  
176 whether model predictions and errors are consistent across these scales. The temporal  
177 dynamics of CH<sub>4</sub> emissions over the season cannot be ignored when calculating long-  
178 term CH<sub>4</sub> budgets (Morin et al., 2014). To investigate the seasonal cycle of CH<sub>4</sub>  
179 emissions in northern wetlands and the underlying processes in a climate model context,  
180 we evaluated and modified the CH<sub>4</sub> biogeochemistry module in the Community Land  
181 Model (CLM 4.5). Seasonal cycles of CH<sub>4</sub> emissions in Alaskan wetlands are analyzed  
182 based on the modified model predictions, CH<sub>4</sub> emission measurements at high-latitude  
183 sites, CarbonTracker CH<sub>4</sub> emission estimates, and atmospheric inversion estimates of  
184 surface CH<sub>4</sub> emissions from data collected in the Carbon in Arctic Reservoirs  
185 Vulnerability Experiment (CARVE). The models and data are described in section 2.  
186 Multi-scale comparison results and discussions are given in section 3, and concluding  
187 remarks in section 4.

## 188 2 Data and Methods

### 189 2.1 Models description

#### 190 2.1.1 CH<sub>4</sub> model in CLM4.5-BGC

191 The CH<sub>4</sub> biogeochemistry model used here (CLM4Me; Riley et al. (2011)) has  
192 been coupled to the revised land model CLM4.5, which includes numerous changes to  
193 vegetation, soil biogeochemistry, and hydrology from the CLM4.0 in which CLM4Me  
194 was originally developed. CLM4Me includes representation of CH<sub>4</sub> production,  
195 oxidation, and transport through the soil column. Transport includes multiple pathways:  
196 aerenchyma transport, ebullition, and aqueous and gaseous diffusion. Aerenchyma is the  
197 most efficient pathway for gas exchange between the soil and atmosphere in wetlands or  
198 aquatic environments, through which atmosphere O<sub>2</sub> is supplied to roots and the  
199 rhizosphere while CH<sub>4</sub> is removed from the soil to shoots and the atmosphere. In  
200 CLM4Me, aerenchyma transport ( $A$ ) is parameterized as gaseous diffusion in response to  
201 a concentration gradient between the soil layer ( $z$ ) and the atmosphere ( $a$ ) as:

202

$$203 \quad A = \frac{C(z) - C_a}{\frac{r_L z}{D_p T \rho_r} + r_a}, \quad (1)$$



204

205 where  $D$  ( $\text{m}^2 \text{s}^{-1}$ ) is the free-air gas diffusion coefficient,  $C(z)$  ( $\text{mol m}^{-3}$ ) is the gaseous  
206 concentration at depth  $z$ , dimensionless  $r_L$  is the ratio of total root length to root depth,  $p$   
207 (-) is tiller porosity;  $T$  ( $\text{m}^2 \text{m}^{-2}$ ) is specific aerenchyma area,  $r_a$  ( $\text{s m}^{-1}$ ) is the aerodynamic  
208 resistance between the surface and the atmospheric reference height, and  $r_r$  (-) is the root  
209 mass fraction in the soil layer. The aerenchyma area  $T$  is seasonally varying with  
210 phenology  $S$  (described below):

211

$$212 \quad T = \frac{f_N N_a S}{0.22} \pi R^2, \quad (2)$$

213

214 where  $N_a$  ( $\text{gC m}^{-2}$ ) is annual net primary production (NPP),  $R$  ( $2.9 \times 10^{-3} \text{ m}$ ) is the  
215 aerenchyma radius,  $f_N$  is the belowground fraction of current NPP, and the factor 0.22 ( $\text{gC}$ )  
216 is the mass of C per tiller. The dimensionless term  $S$  is included in CLM4Me to capture  
217 seasonal cycles of aerenchymous tissues. In the absence of data on phenology of  
218 aerenchyma,  $S$  was originally taken as the leaf area index (LAI).

219 The default method for calculating inundation fraction ( $F_{def}$ ) remains the same as  
220 described in Riley et al. (2011), which applied a simple inversion model to represent the  
221 spatial inundation:

222

$$223 \quad F_{def} = p_1 e^{-z_w/p_2} + p_3 Q_r, \quad (3)$$

224

225 The three parameters ( $p_1, p_2, p_3$ ) are optimized with the inundation map by Prigent et al.  
226 (2007).  $z_w$  is simulated water table depth (m) and  $Q_r$  is surface runoff ( $\text{mm s}^{-1}$ ). We also  
227 applied an estimate of inundation fraction  $F_{S+G}$  (Poulter et al., In Review) derived from  
228 seasonal cycle of inundation fraction from the Surface Water Microwave Product Series  
229 Version 2.0 (SWAMPS, Schroeder et al., 2015) developed at the NASA Jet Propulsion  
230 Laboratory with the Global Lakes and Wetlands Dataset (GLWD, Lehner and Doll, 2004)  
231 to discuss the potential uncertainties in  $\text{CH}_4$  emissions caused by wetland area.

232 Our model is driven by half-degree CRUNCEP V5 6-Hourly Atmospheric  
233 Forcing dataset (1901-2013) (<http://dods.extra.cea.fr/data/p529viov/cruncep/readme.htm>).  
234 Monthly wetland  $\text{CH}_4$  emissions are simulated between the year 2000 and 2012 during  
235 which  $F_{S+G}$  is available. The monthly  $\text{CH}_4$  emissions in half-degree resolution are  
236 regridded to  $1^\circ \times 1^\circ$  and averaged longitudinally to compare with CarbonTracker predicted  
237  $\text{CH}_4$  fluxes. Daily wetland  $\text{CH}_4$  emissions are simulated for year 2012 and 2013 to  
238 calculate the atmospheric enhancements of  $\text{CH}_4$  due to modeled surface emissions.

239

## 240 2.1.2 WRF-STILT modeling of $\text{CH}_4$ transport

241 We simulate the atmospheric CH<sub>4</sub> mole fraction enhancements due to wetland  
242 emissions by combining the CLM4.5 predicted daily surface emissions with the land  
243 surface influences (“footprint”) calculated by the Weather Research and Forecasting-  
244 Stochastic Time-Inverted Lagrangian Transport (WRF-STILT) model (Henderson et al.,  
245 2015). WRF-STILT estimates the upwind surface influence along the flight track of the  
246 CARVE aircraft by releasing 500 particles at the point of flight measurement and  
247 allowing them to stochastically disperse in reverse time over 10 days (Henderson et al.,  
248 2015). The resolution of the resulting footprint sensitivity used in this study  
249 is 0.5 °×0.5°, covering 30-90°N, circumpolar. However, we assume that CH<sub>4</sub>  
250 transported from areas outside of Alaska are most likely mixed thoroughly in the  
251 atmosphere before they reach Alaska, and therefore only contribute to the background  
252 abundance of CH<sub>4</sub>.

## 253 **2.2 Measurements of CH<sub>4</sub>**

### 254 **2.2.1 Site-Scale Observations**

255 We compare CLM4.5 CH<sub>4</sub> emission predictions with data obtained from  
256 published studies and recent measurements of northern hemisphere static chamber (SC)  
257 measurements at 10 sites and eddy covariance (EC) measurements at 10 sites, of which 8  
258 are in Alaska (Supplement Table S1). The eddy covariance measurements in Alaska (Fig.  
259 S2) are obtained at the Barrow Environmental Observatory (BEO1) tower operated by the  
260 Next Generation Ecosystem Experiment (NGEE)-Arctic group; Barrow Environmental  
261 Observatory tower (BEO2), Biocomplexity Experiment South (BES) tower, Climate  
262 Monitoring and Diagnostics Laboratory (CMDL) tower, Atqasuk (ATQ) tower and  
263 Ivotuk (IVO) tower operated by Global Change Research Group at San Diego State  
264 University (Zona et al., 2016); tower in Fairbanks (FAI, Iwata et al., 2015) operated by  
265 International Arctic Research Center, the University of Alaska Fairbanks; and tower at  
266 the Imnavait Creek watershed (IMN, Euskirchen et al., 2012). Monthly means are  
267 calculated across each observational record to compare to predicted mean seasonal CH<sub>4</sub>  
268 cycle. We discarded the monthly mean if the number of valid measurement days is less  
269 than half a month.

### 270 **2.2.2 Comparisons to Airborne Measurements**

271 The regionally integrated CH<sub>4</sub> mole fraction enhancements over Alaska were  
272 calculated from the CH<sub>4</sub> mole fractions measured by NOAA and Harvard Picarro  
273 spectrometers aboard a NASA C-23B aircraft (N430NA) during CARVE aircraft flights  
274 (Chang et al., 2014). The Harvard CH<sub>4</sub> measurements were gap filled with the NOAA  
275 CH<sub>4</sub> measurements to create a continuous 5-s time series. The flight measurements were  
276 conducted on selected days from May to September in 2012 and April to October in 2013  
277 during the Carbon in Arctic Reservoirs Vulnerability Experiment (CARVE) campaign,  
278 for a total of 31 flight days in 2012 and 43 flight days in 2013 (Fig. S1 and Table S2).  
279 The measurements of CH<sub>4</sub> with concurrent CO mole fractions above 150 ppb are  
280 excluded to remove possible CH<sub>4</sub> production from biomass burning. In Alaska,  
281 atmospheric boundary layer depth is in the range of 1100-1600 m above ground level  
282 (agl) during April and October according to COSMIC satellite and Radiosonde data

283 (Chan and Wood, 2013). We assume that the observed concentration fluctuations below  
284 500m agl can be used to infer the variation of surface CH<sub>4</sub> fluxes; the measurements  
285 above 1600 m agl are used to infer background mole fraction of CH<sub>4</sub>. The monthly mean  
286 enhancements in observed atmospheric CH<sub>4</sub> mole fraction is compared to that estimated  
287 from the CLM4.5 CH<sub>4</sub> enhancements.

### 288 2.2.3 Comparisons to Global-Scale Inversions

289 To compare our methane emissions with global and regional scale inversions, we  
290 use monthly regional CH<sub>4</sub> emissions predicted by CarbonTracker (Peters et al., 2007;  
291 Bruhwiler et al., 2014) at 1°×1° resolution. In CarbonTracker estimates, the natural CH<sub>4</sub>  
292 emissions correspond to wetlands, soils, oceans, insects, and wild animals. To examine  
293 the land CH<sub>4</sub> emissions only, we apply the CLM land mask to exclude the inferred  
294 CarbonTracker CH<sub>4</sub> emission from the ocean surface. CarbonTracker CH<sub>4</sub> estimates are  
295 available from January 2000 through December 2010; we therefore limit comparisons  
296 against the CLM4.5 predictions to this period.

## 297 3 Results and Discussion

### 298 3.1 Model constraints and comparison with observations

299 We performed sensitivity analyses of all the parameters affecting seasonal CH<sub>4</sub>  
300 production, oxidation, and emission pathways and found that the parameterization of  
301 aerenchyma transport has the greatest impact on the seasonal CH<sub>4</sub> emissions in saturated  
302 areas. The CH<sub>4</sub> surface flux sensitivity to aerenchyma is most sensitive to aerenchyma  
303 area in saturated conditions, and decreases with increasing aerenchyma area, because  
304 increased O<sub>2</sub> fluxes through aerenchyma cause more CH<sub>4</sub> oxidation in the rhizosphere  
305 (Riley et al., 2011). Meng et al. (2012) tested plant functional type (pft)-specific fine root  
306 carbon ( $C_{FR}$ ) as a proxy of aerenchyma area and found that aerenchyma area dependence  
307 on  $C_{FR}$  leads to about 39% increases in global annual CH<sub>4</sub> emissions. In that study, an  
308 early spring spike in CH<sub>4</sub> emission through aerenchyma transport was shown at a  
309 Michigan site in both LAI and  $C_{FR}$  based aerenchyma area. Our analysis shows that the  
310 simulated CH<sub>4</sub> burst through aerenchyma transport during spring thaw is very common in  
311 areas experiencing winter dormancy. In CLM4.5, CH<sub>4</sub> production in a given volume of  
312 soil is proportional to heterotrophic respiration (HR) in that soil volume, adjusted by soil  
313 temperature, pH, redox potential, and variation of seasonal inundation fraction. In the  
314 model, CH<sub>4</sub> production starts when the soil temperature is above the freezing point.  
315 However, CLM4.5 LAI lags behind the primary thaw day, which, because the original  
316 representation of aerenchyma in CLM4.5 is tied directly to LAI, results in a very low  
317 aerenchyma area and thus low aerenchyma transport of O<sub>2</sub> into the soil during spring  
318 thaw period. Only a very small portion of the CH<sub>4</sub> produced in the soil column is  
319 oxidized, allowing a large fraction of CH<sub>4</sub> to be transported to the surface by aerenchyma.  
320 The low oxidation rate also occurs when aerenchyma area is calculated with  $C_{FR}$ .

321 The uncertainty in representing the seasonality of aerenchyma area is due to (1)  
322 poor current understanding of root dynamics and their control on aerenchyma area and (2)  
323 scant relevant observations. In tundra, the aboveground production is often not a good

324 proxy for belowground production, because the soil temperature peaks later in the  
325 growing season than solar irradiance (Sullivan and Welker, 2005; Sloan, 2011). Further,  
326 root dynamics are strongly species dependent. Root growth of *Eriophorum angustifolium*  
327 may not be delayed when soil temperature is near 0°C (Chapin, 1974; Billing et al., 1977),  
328 while *Dupontia Fischeri* produces many fewer root tips at these low temperatures. In  
329 *Eriophorum vaginatum*, fine root growth is lagged significantly behind the aboveground  
330 spring growth flush (Kummerow and Russell, 1980).

331 To eliminate the possible bias in the seasonal variation of roots and the extremely  
332 low oxidation rate which caused CLM4.5 to predict a large CH<sub>4</sub> burst from inundated  
333 areas during the spring thaw, we modified the model parameter  $S$  to be constant, which is  
334 used in the aerenchyma area estimation. We constrained  $S$  using global total CH<sub>4</sub>  
335 emissions estimated by top-down and bottom-up simulations during 2000-2009 (Kirschke  
336 et al., 2013) and site-level measurements. We exclude the CH<sub>4</sub> emission from non-  
337 inundated areas for the analysis of seasonal dynamics because the model shows very  
338 small seasonal contribution of CH<sub>4</sub> emissions from non-inundated areas globally (Fig. 1).  
339 This CH<sub>4</sub> emission pulse from non-inundated areas, which may be related to soil moisture  
340 anomalies during spring thaw, has not been experimentally validated, but can lead to  
341 large biases in simulated CH<sub>4</sub> emissions from northern high latitudes (>50°N) in May and  
342 June (Fig. 1a and 1b). This simplification of the model produced seasonal cycles that did  
343 not contain the large springtime CH<sub>4</sub> emission bursts, and we therefore used this modified  
344 version for all experiments here.

345 We assessed the sensitivity of the modeled CH<sub>4</sub> fluxes to parametric uncertainty  
346 in the constant dimensionless factor  $S$ , as described above.  $S$  has a direct effect on the  
347 magnitude of modeled CH<sub>4</sub> emissions via its control of oxygen diffusion through the soil  
348 column and thus CH<sub>4</sub> oxidation. When  $S = LAI$ , the very low  $LAI$  in the spring thaw  
349 period leads to low oxidation and consequently overestimated CH<sub>4</sub> net emissions  
350 compared to CarbonTracker predictions. During the growing season, the model  
351 overestimates  $LAI$  at high latitude (Tian et al., 2004) leading to high oxidation and  
352 consequently underestimated net CH<sub>4</sub> emissions (Fig. 1e and f). However, few  
353 observations of aerenchymous tissue biomass are available to provide an *a priori*  
354 constraint to this value. Our goal here is to use a reasonable value of this parameter, not  
355 to fully characterize the uncertainty of the parameter choice on CH<sub>4</sub> emissions.

356 Based on a comparison of the globally integrated CH<sub>4</sub> flux with other global  
357 estimates, we choose  $S=4$ , which resulted in an estimated annual total CH<sub>4</sub> emission of  
358 228 [Inter-annual Variability (IAV): 221- 239] Tg CH<sub>4</sub> yr<sup>-1</sup> with  $F_{def}$  and 206 [IAV: 200-  
359 217] Tg CH<sub>4</sub> yr<sup>-1</sup> with  $F_{S+G}$  during the period 2000 - 2009. The top-down and bottom-up  
360 models provide estimates of CH<sub>4</sub> emissions from natural wetlands of 175 [IAV: 142-208]  
361 Tg CH<sub>4</sub> yr<sup>-1</sup> and 217 [IAV: 177-284] Tg CH<sub>4</sub> yr<sup>-1</sup>, respectively, during the same period  
362 (Kirschke et al., 2013). The mean CH<sub>4</sub> emission predicted by CLM4.5 is about 42 Tg  
363 CH<sub>4</sub> yr<sup>-1</sup> lower than the original CLM4Me prediction (annual mean of 270 Tg CH<sub>4</sub> yr<sup>-1</sup>  
364 from 1948 to 1972), but slightly larger than the mean value from other bottom-up and  
365 top-down models. The disagreement between studies with different models is as large as  
366 66% (Kirschke et al., 2013), hence our estimate is well within the range of values from  
367 top-down constraints and underscores the uncertainty involved in using such a constraint  
368 in inferring model parameters.

369 Compared with CarbonTracker predictions, CLM's biases of underestimated  
370 growing-season CH<sub>4</sub> emissions north of 56°N and biases of overestimated CH<sub>4</sub> emissions  
371 in 2-53°N and 34-56°S are reduced when using  $S = 4$  compared to the default  
372 parameterization (Fig. 1d and f). For the global zonal mean, the CLM CH<sub>4</sub> prediction  
373 biases are reduced with  $F_{S+G}$  (RMSE=2.5 mg CH<sub>4</sub> m<sup>-2</sup> day<sup>-1</sup>) compared with  $F_{def}$  (RMSE  
374 = 3.1 mg CH<sub>4</sub> m<sup>-2</sup> day<sup>-1</sup>). With  $F_{S+G}$ , the biases are much reduced in 2-50°N and 30-58°S.  
375 However, negative CH<sub>4</sub> emission biases in the tropics remain (Fig. 1c and 1e). The  
376 differences in CH<sub>4</sub> emissions using SWAMPS-GLWD and CLM4.5 predicted inundation  
377 fraction implies that the prediction uncertainties are not only from the biogeochemical  
378 parameterization but also from the wetland extent, consistent with several recent model  
379 inter-comparison analyses (Melton et al., 2013; Bohn et al., 2015). In Alaska, the  
380 predicted annual CH<sub>4</sub> emissions between 2000 and 2010 are 1.47±0.20, 1.58±0.07, and  
381 1.12±0.05 Tg CH<sub>4</sub> yr<sup>-1</sup> for CarbonTracker, CLM4.5 with  $F_{S+G}$ , and CLM4.5 with  $F_{def}$ ,  
382 respectively. Although our predicted annual emissions are reasonable compared with  
383 most land surface model predictions, the May to September predictions are about 50-70%  
384 of the emissions estimated using an atmospheric inversion based on CARVE observations  
385 of 2.1± 0.5 Tg CH<sub>4</sub> yr<sup>-1</sup> (Chang et al., 2014).

## 386 3.2 Seasonal CH<sub>4</sub> emissions

### 387 3.2.1 Site level comparison

388 The mean seasonal cycle of predicted CH<sub>4</sub> emissions is calculated from the 2000-  
389 2012 monthly mean in a 0.5°×0.5° grid cell where site measurements exist, while the  
390 seasonal cycle of site measurements is calculated for the measurement years. If multiple  
391 measurement sites and multiple measurement years with the same measurement method  
392 (SC or EC) exist within a given grid cell, the observations are averaged to create a grid  
393 cell mean value that can be directly compared with the modeled value for that grid cell. In  
394 the 10 site-level static chamber measurements at saturated sites (Fig. 2a-l), the seasonality  
395 is well predicted by the revised CLM4.5 CH<sub>4</sub> model at most sites. Measurements and  
396 predictions show the peak emission month to be July or August at most sites, except the  
397 site in Michigan, USA (Fig. 2f) where the model successfully predicted the peak  
398 emissions in May. However, the model misrepresents the seasonality at the Stordalen  
399 (Sweden) (Fig. 2a and k) and the Boreas NSA (Canada) (Fig. 2i) site. At the Ruorgai  
400 (China) (Fig. 2j), the model does not show a strong seasonal variation from April to  
401 September, and notably underestimates the growing season CH<sub>4</sub> emissions. The  
402 underestimation of growing season emissions is also found in the Minnesota (USA),  
403 Michigan (USA), and Boreas NSA (Canada) sites (Fig. 2d, 2e, 2f and 2h). The sites  
404 experiencing soil frost with valid measurements in the cold season demonstrate the  
405 CLM4.5 underestimation of CH<sub>4</sub> emissions during this period (Fig. 2a, 2d, 2e and 2i).

406 The eddy covariance measurements from four sites, the BEO1, BEO2, BES, and  
407 CMDL sites are in the same model grid cell, therefore, the measurements in these four  
408 sites are aggregated to the same grid cell as that of Alaska (Fig. 2m). As the footprints of  
409 the measurement towers were not estimated, all the modeled CH<sub>4</sub> emissions at eddy  
410 covariance sites are weighted with an observationally estimated seasonal-invariant range  
411 of inundation fraction: Stordalen: 80-100%; Boreas SSA: 50-90%; Barrow: 60-100%;

412 Atqasuk: 10-30%; Ivotuk: 5-25%; Fairbanks: 0.5-2.5% and IMN: 5-25%. Measurements  
413 at the Stordalen site (Fig. 2a and k) show very different CH<sub>4</sub> emission patterns in  
414 seasonality and magnitude for different years and measurement methods. The model  
415 significantly underestimates CH<sub>4</sub> emissions even with the maximum fraction of  
416 inundation in Stordalen (Fig. 2k). In comparison with the static chamber measurements at  
417 Alaska (Fig. 2h), the model predicts a much shorter CH<sub>4</sub> emission season at the non-  
418 inundated sites (Fig. 2m-q). The estimated CH<sub>4</sub> emissions begin in April at Ivotuk,  
419 Fairbank, and Imnavait. At the northern sites, Barrow and Atqasuk, the estimated CH<sub>4</sub>  
420 emissions begin in May. In the short emission season, the model underestimates CH<sub>4</sub>  
421 emissions in June and July at Barrow and Atqasuk and in July at Imnavait, even with the  
422 maximum inundation estimation. While the cold-season measurements at Barrow,  
423 Atqasuk, and Ivotuk show large CH<sub>4</sub> emissions from October to April in agreement with  
424 the static chamber measurements at the sites with cold season soil frost, predicted CH<sub>4</sub>  
425 emissions end in October at all the Alaskan sites. The largest monthly mean emissions in  
426 Alaska cold season are 24.8±9.0 mg CH<sub>4</sub> m<sup>-2</sup> day<sup>-1</sup> measured in October at Ivotuk.

427 A number of factors affect the correspondence between site-level CH<sub>4</sub> emission  
428 observations and CLM4.5 predictions (Fig. 2), including: (1) we used reanalysis climate  
429 forcing data which may lead to some of the differences with the site observations; (2) we  
430 used the model's default surface characterization, which is unlikely to exactly match the  
431 actual vegetation and soil properties; (3) the spatial and temporal coverage of the site data  
432 are sparse; (4) the inter-annual variation of wetland CH<sub>4</sub> emission can be significant; (5)  
433 the method of measuring CH<sub>4</sub> fluxes varied from site to site and (6) the seasonal fraction  
434 of inundation in eddy covariance tower footprint is unknown. We also expect differences  
435 between our CLM4.5 predictions and those reported in Riley et al., (2011) at the site-  
436 level comparison, because: (1) simulations in this study were done at higher resolution  
437 (0.5°x0.5°) than those in Riley et al. (2011) (1.9° x2.5°); (2) the current simulations are  
438 forced by CRUNCEP climate, while Riley et al., (2011) simulations were forced with  
439 Qian et al., (2006) climate; (3) the *S* parameter is changed, as discussed above; and (4)  
440 the overall water and carbon cycles of CLM changed substantially between CLM4.0 and  
441 CLM4.5 (Koven et al., 2013). The site-level discrepancies occur because of the  
442 uncertainties discussed above and those arising from other parameters (Riley et al., 2011),  
443 including: Q<sub>10</sub> of CH<sub>4</sub> production and oxidation, CH<sub>4</sub> half-saturation oxidation coefficient,  
444 O<sub>2</sub> half-saturation oxidation coefficient, maximum oxidation rate of CH<sub>4</sub> oxidation, and  
445 impact of pH and redox potential on CH<sub>4</sub> production.

### 446 3.2.2 Regional CH<sub>4</sub> emissions comparison

447 The biases between CLM4.5 and CarbonTracker CH<sub>4</sub> emissions vary with latitude  
448 (Fig. 3). The aggregated  $F_{S+G}$  led to larger CH<sub>4</sub> emission biases in Alaska (RMSE = 4 mg  
449 CH<sub>4</sub> m<sup>-2</sup> day<sup>-1</sup>) compared to the CH<sub>4</sub> prediction with  $F_{def}$  (RMSE = 3 mg CH<sub>4</sub> m<sup>-2</sup> day<sup>-1</sup>),  
450 although it led to smaller global CH<sub>4</sub> emission biases. In Alaska between 58-66°N during  
451 the growing season, CLM4.5 using  $F_{def}$  has good agreement with CarbonTracker  
452 predictions. In this region, CH<sub>4</sub> emissions begin in May, peak in July and August, and  
453 end in October (Fig. 4). In May and June, CarbonTracker shows a weak CH<sub>4</sub> sink (~O[10<sup>-2</sup>-  
454 10<sup>-1</sup>] mg CH<sub>4</sub> m<sup>-2</sup> day<sup>-1</sup>) in contrast to a CLM4.5 predicted weak CH<sub>4</sub> source (~O[10<sup>-1</sup>]  
455 mg CH<sub>4</sub> m<sup>-2</sup> day<sup>-1</sup>) with  $F_{def}$  and stronger CH<sub>4</sub> source (~O[1] mg CH<sub>4</sub> m<sup>-2</sup> day<sup>-1</sup>) with  $F_{S+G}$



456 in the interior region of Alaska (Interior Alaska) between 63°N-66°N . We hypothesize  
457 that this discrepancy occurs because of the difference in the two wetland datasets and the  
458 accounting of CH<sub>4</sub> emissions from the non-inundated areas in CarbonTracker. Net CH<sub>4</sub>  
459 consumption occurs at dry sites where oxygen is available in the top soil layers  
460 (Wickland et al., 1999); however, CH<sub>4</sub> fluxes from the non-inundated areas which could  
461 be substantial (Zona et al., 2016) are excluded in CLM4.5 predictions shown in Fig. 3, as  
462 described in Methods. Interior Alaska has a highly continental climate with warm and  
463 relatively dry summers and extremely cold winters. The weak CH<sub>4</sub> source in the dry  
464 summer is thus caused by a reduced wetland extent in Interior Alaska. Interior Alaska  
465 experiences the most rain events in autumn, mainly in August and September (Hinzman  
466 et al., 2006), which restores some of the extent of wetlands and leads to increases in CH<sub>4</sub>  
467 emissions in August and early September. CarbonTracker successfully represented the  
468 restored wetland in August and September but not CLM4.5 (Fig. 3 and 4). The autumn  
469 emission period is very short and ends with the onset of winter, resulting in a strong drop  
470 in CH<sub>4</sub> emissions in October.

471 The CLM4.5 underestimation of northern (> 68°N) Alaska site-level CH<sub>4</sub>  
472 emissions during the growing season at some sites is confirmed with comparison to  
473 CarbonTracker inversions (Fig. 3b). In southern and northern coastal Alaska, CLM4.5  
474 predicts a much shorter CH<sub>4</sub> emission season and a smaller magnitude of CH<sub>4</sub> emissions  
475 than CarbonTracker. The **period of the largest** underestimation by CLM4.5 is from May  
476 to July with the maximum underestimation of about 9.2 mg CH<sub>4</sub> m<sup>-2</sup> day<sup>-1</sup> in June. The  
477 underestimated CH<sub>4</sub> emissions occur with both  $F_{S+G}$  and  $F_{def}$  in the north of 68°N.  
478 During the cold season from October to April, CLM4.5 predictions with  $F_{S+G}$  or  $F_{def}$  are  
479 consistently smaller than CarbonTracker estimates across all the latitudes. The mean  
480 underestimation of cold season CH<sub>4</sub> emission is less than 1 mg CH<sub>4</sub> m<sup>-2</sup> day<sup>-1</sup>, which is  
481 much smaller than the underestimation we found compared to site level measurements.  
482 In comparison with CarbonTracker, CLM4.5 predicted 0.46±0.07Tg and 0.39±0.08Tg  
483 less Alaska wide CH<sub>4</sub> emissions in cold season (October to April) with  $F_{S+G}$  and  $F_{def}$ ,  
484 respectively.

485 The CarbonTracker inversions suggest 21.9±3.2% of the annual Alaska CH<sub>4</sub>  
486 emissions occur during the cold season, while CLM4.5 predicts only 3.5±1.3% and  
487 8.3±3.0% (with  $F_{def}$  and  $F_{S+G}$ , respectively) occur during the cold season. When  
488 September and April are included in the “cold season”, the contribution is increased to  
489 45.3±4.5% by CarbonTracker, which is slightly smaller than the cold season contribution  
490 (50±9%) inferred from site-level (BEO2, BES, CMDL, ATQ and IVO) measurements  
491 (Zona et al., 2016). The September-April contributions to annual emissions predicted by  
492 CLM4.5 are 32.1±8.1% and 40.1±14.7% of the predicted annual emissions with  $F_{S+G}$  and  
493  $F_{def}$ , respectively. Although CH<sub>4</sub> fluxes from the ocean surface are excluded, we cannot  
494 exclude some influence of coastal grid cells on the CarbonTracker estimates.

495 The atmospheric CH<sub>4</sub> mole fraction enhancements calculated from CLM4.5  
496 predicted CH<sub>4</sub> emissions are lower than the CARVE measured CH<sub>4</sub> mole fraction  
497 enhancements (Fig. 5). However, in contrast to the emission underestimations that only  
498 occur from May to July, the monthly atmospheric CH<sub>4</sub> mole fraction enhancements are  
499 underestimated throughout the year, with a maximum underestimation in August (Fig. 5a).  
500 The CARVE measured peak mole fraction enhancement due to surface CH<sub>4</sub> emissions is

501 in August for both 2012 and 2013. Although CLM4.5 predicted the peak CH<sub>4</sub> mole  
502 fraction enhancement in August, 2012, predicted seasonal CH<sub>4</sub> mole fraction  
503 enhancements are much smaller in 2013 and peaks in September. The underestimation of  
504 cold season mole fraction CH<sub>4</sub> enhancements by CLM4.5 leads to 24.0±9.2 ppb and  
505 18.9±17.3 ppb lower CH<sub>4</sub> mole fraction enhancements in April and October 2013,  
506 respectively. From April to October, the two-year mean monthly atmospheric CH<sub>4</sub> mole  
507 fraction enhancements are underestimated by 15 ppb in WRF-STILT-CLM model  
508 predictions. The underestimation may not be attributed to anthropogenic CH<sub>4</sub> source and  
509 agricultural waste because: (1) we excluded both observed and modeled CH<sub>4</sub> mole  
510 fraction enhancements when [CO]>150 ppb, given that anthropogenic CH<sub>4</sub> mole fraction  
511 enhancements are consistently correlated to CO mole fraction enhancements (Zona et al.,  
512 2016) and (2) The CH<sub>4</sub> emissions from agricultural waste does not show strong seasonal  
513 variation according to CarbonTracker estimates. The large standard deviation of CARVE  
514 observed CH<sub>4</sub> mole fraction enhancements implies that the CH<sub>4</sub> emissions have large  
515 spatial and temporal variability. The CLM4.5 predictions are generally within the  
516 observed range of variation except in April and May in 2013.

517 The very low cold season CH<sub>4</sub> emission predictions at site and regional scales  
518 occurs because of the assumed temperature sensitivity for CH<sub>4</sub> production when the soil  
519 temperature of a given layer is at or below freezing (i.e., no CH<sub>4</sub> production occurs in that  
520 soil layer). The multi-layer structure of CLM4.5 can in principle generate CH<sub>4</sub> emissions  
521 deeper in the soil after the surface has frozen, though even then, modeled diffusion rates  
522 through frozen surface layers are low. Although the measurements show winter CH<sub>4</sub>  
523 emissions, it remains uncertain whether these emissions are from production at low  
524 temperature or residual CH<sub>4</sub> from the end of the growing season. Understanding which of  
525 these is occurring is important for diagnosing how to improve model representation of the  
526 processes responsible for the wintertime fluxes. The cold season underestimation by  
527 CLM4.5 is also partly attributed to the low wetland area during this period at high  
528 latitudes (currently,  $F_{def}$  is set to zero when snow is present). Given the current  
529 observations of CH<sub>4</sub> emissions during the cold season, we believe these two factors need  
530 to be re-evaluated in CLM4.5.

### 531 3.3 Interannual variation of CH<sub>4</sub> cycle

532 The CLM4.5 simulated Alaska CH<sub>4</sub> emissions using  $F_{def}$  are in very good  
533 agreement with CarbonTracker-CH<sub>4</sub> emission in the growing season but biased in the  
534 cold season (Fig. 6). The largest growing season discrepancies occur in 2006 and 2007.  
535 Bruhwiler et al. (2014) attributed the CarbonTracker 2007 CH<sub>4</sub> emission anomaly to  
536 warmer temperatures and higher than normal precipitation. However, the CRUNCEP  
537 reanalysis data we used to force CLM4.5 do not have a positive precipitation anomaly in  
538 either 2006 or 2007 (Fig. 7a). In contrast, there is a strong negative precipitation  
539 anomaly in 2007. The obvious wet years (2000, 2005, 2008, 2011 and 2012) in the  
540 CRUNCEP reanalysis data are not directly related to the predicted and measured wetland  
541 area anomaly or CH<sub>4</sub> emission anomaly. The mean air temperature in 2007 is only  
542 slightly higher than 2000-2012 mean air temperature (Fig. 7b). The correlation analysis  
543 implies that the model predicted interannual CH<sub>4</sub> variation is mainly explained by  
544 temperature variation (Fig. 8a,  $r=0.86$ ,  $P=0.0007$ ), followed by the default wetland extent  
545 ( $F_{def}$ ) variation (Fig. 8b,  $r=0.65$ ,  $P=0.03$ ), but weakly explained by SWAMPS-GLWD

546 wetland extent ( $F_{S+G}$ ) variation ( $r=0.44$ ,  $P=0.17$ ) and precipitation variation ( $r=0.18$ ,  
547  $P=0.58$ ). When the  $\text{CH}_4$  predictions are calculated with  $F_{S+G}$ , correlation between the  
548 interannual variation of  $\text{CH}_4$  and variation in  $F_{S+G}$  ( $r=0.18$ ,  $P=0.59$ ), precipitation ( $r=0.36$ ,  
549  $P=0.29$ ), and temperature ( $r=0.32$ ,  $P=0.33$ ) are substantially reduced. Interannual  
550 variation of  $\text{CH}_4$  emissions by CarbonTracker are not well correlated to SWAMPS-  
551 GLWD wetland extent variation ( $r=0.33$ ,  $P=0.32$ ), variations in CRUNCEP temperature  
552 ( $r=-0.23$ ,  $P=0.49$ ), or precipitation ( $r=-0.06$ ,  $P=0.86$ ).

#### 553 **4 Concluding remarks**

554 We implemented and tested needed changes to the estimate of aerenchyma area in  
555 CLM4.5. The modeled and measured  $\text{CH}_4$  emissions and enhancements in atmospheric  
556 mole fractions of  $\text{CH}_4$  are used to analyze the seasonal wetland  $\text{CH}_4$  emission cycle in  
557 Alaska. Both the measurements and model predictions show large latitudinal variability  
558 of  $\text{CH}_4$  seasonal cycles. At the site level, CLM4.5 generally captures the seasonality in  
559 growing season  $\text{CH}_4$  emissions. However, comparing eddy covariance  $\text{CH}_4$  observations  
560 with the model predictions is complicated by the unknown fraction of inundation in the  
561 footprint of the measurement tower, which may cause large variations in  $\text{CH}_4$  emission  
562 predictions. Measurements from the sites experiencing wintertime soil frost imply that  
563  $\text{CH}_4$  emissions continue in the cold season (October to April). The likely incorrect  
564 treatment of  $\text{CH}_4$  production under soil frost in CLM4.5 leads to underestimates of the  
565 wintertime emissions. This conclusion is confirmed by the discrepancies between  
566 CLM4.5 and CarbonTracker predictions, although the cold season discrepancies between  
567 CLM4.5 and CarbonTracker are much smaller than the discrepancies between CLM4.5  
568 and site-level measurements. The differences between the seasonality predicted by  
569 CLM4.5 and CarbonTracker vary with time and latitude, although the Alaska area-  
570 integrated  $\text{CH}_4$  emissions agree well. Besides the strength of wintertime  $\text{CH}_4$  emissions,  
571 the main discrepancies between CLM4.5 and CarbonTracker estimates are northern and  
572 southern coastal area  $\text{CH}_4$  emissions. The inundation area leads to uncertainties in  
573 predictions of seasonal and interannual variability of  $\text{CH}_4$  emissions. Compared with the  
574 CLM4.5 predicted inundation area, the aggregated  $F_{S+G}$  inundation led to smaller global  
575  $\text{CH}_4$  emission biases than  $F_{def}$  (RMSE dropped from  $3.1 \text{ mg CH}_4 \text{ m}^{-2} \text{ day}^{-1}$  to  $2.5 \text{ mg CH}_4$   
576  $\text{m}^{-2} \text{ day}^{-1}$ ) between CLM4.5 and CarbonTracker. In contrast, the  $F_{S+G}$  inundation area  
577 increased seasonal emission biases in Alaska by increasing RMSE from 3 to 4  $\text{mg CH}_4 \text{ m}^{-2}$   
578  $\text{day}^{-1}$  compared with the CLM4.5 predicted inundation. The larger SWAMPS-GLWD  
579 inundation area leads to much stronger Alaska wide annual  $\text{CH}_4$  emissions compared to  
580 those calculated from the default predicted inundation area. CLM4.5 predictions show  
581 that the interannual variations of  $\text{CH}_4$  emissions are correlated with the reanalysis air  
582 temperature and wetland extent variation. In contrast, interannual variation in  
583 CarbonTracker  $\text{CH}_4$  emissions is weakly related to interannual variation in SWAMPS-  
584 GLWD wetland area and reanalysis precipitation and temperature.

585 The CLM4.5  $\text{CH}_4$  module constrained from global total annual  $\text{CH}_4$  emissions  
586 does not accurately represent the seasonal cycles at the regional and site scale seasonal  
587 cycles due to large temporal and spatial heterogeneity in surface  $\text{CH}_4$  emissions and  
588 wetland extent. Further improving the  $\text{CH}_4$  biogeochemical model at the seasonal and  
589 annual time scales requires further extensive experiments to better understand climate  
590 controls on above- and below-ground physiological processes and how vegetation

591 controls gaseous transport (e.g. CH<sub>4</sub> production under low temperatures). Although cold  
592 season site-level measurements are rare, the large discrepancies in winter emissions  
593 between CLM4.5 and CarbonTracker predictions and site measurements indicate that  
594 studies on winter ecosystem activities and wetland evolution in high latitude would be  
595 valuable.

596

597

598 **Acknowledgements:** Funding for this study was provided by the US Department of  
599 Energy, BER, under the RGCM program and NGEE-Arctic project under contract # DE-  
600 AC02-05CH11231. We thank the CARVE flight group for efforts on CARVE science  
601 flights. CarbonTracker CH<sub>4</sub> results provided by NOAA ESRL, Boulder, Colorado, USA  
602 from the website at <http://www.esrl.noaa.gov>. The eddy covariance tower data used in  
603 this study were supported by the Division of Polar Programs of the National Science  
604 Foundation (NSF) (Award 1204263); Carbon in Arctic Reservoirs Vulnerability  
605 Experiment (CARVE), an Earth Ventures (EV-1) investigation, under contract with the  
606 National Aeronautics and Space Administration; and Department of Energy (DOE) Grant  
607 DE-SC005160. Logistical support was funded by the NSF Division of Polar Programs.  
608

609

## References

- 610 Alavala, P. C. and Kirchoff, V. W. J. H.: Methane fluxes from the Pantanal floodplain in  
611 Brazil: Seasonal variation, in: *Non-CO<sub>2</sub> Greenhouse Gases: Scientific understanding,*  
612 *control and implementation*, edited by: Goossens, A., De Visscher, A., Boeckx, P., and  
613 Van Cleemput, O., Kluwer Academic Publishers, Netherlands, 95–99, 2000.
- 614 Bartlett, K. B., Crill, P. M., Sass, R. L., Harriss, R. C., Dise, N. B.: Methane emissions  
615 from tundra environments in the Yukon-Kuskokwim delta, Alaska, *J. Geophys. Res.*,  
616 97D, 16645–16660, 1992.
- 617 Bergamaschi, P., Frankenberg, C., Meirink, J. F., Krol, M., Villani, M. G., Houweling, S.,  
618 Dentener, F., Dlugokencky, E. J., Miller, J. B., Gatti, L. V., Engel, A., and Levin, I.:  
619 Inverse modeling of global and regional CH<sub>4</sub> emissions using SCIAMACHY satellite  
620 retrievals, *J. Geophys. Res.-Atmos.*, 114, D22301, doi:10.1029/2009JD012287, 2009.
- 621 Billings, W. D., Peterson, K. M., Shaver, G. R., Trent, A. W.: Root growth, respiration,  
622 and carbon dioxide evolution in an Arctic tundra soil. *Arctic Alpine Res.*, 9, 129–137,  
623 1977.
- 624 Bohn, T. J., Melton, J. R., Ito, A., Kleinen, T., Spahni, R., Stocker, B. D., Zhang, B., Zhu,  
625 X., Schroeder, R., Glagolev, M. V., Maksyutov, S., Chen, G., Denisov, S. N., Eliseev,  
626 A. V., Gallego-Sala, A., McDonald, K. C., Rawlins, M. A., Subin, Z. M., Tian, H.,  
627 Zhuang, Q., Kaplan, J. O.: WETCHIMP-WSL:intercomparison of wetland methane  
628 emissions models over West Siveria, *Biogeosciences*, 12, 3321-3349, 2015.
- 629 Brouchkov, A., Fukuda, M., Tomita, F., Asano, K., Tanaka, M.: Microbiology and gas  
630 emission at low temperatures: some field and experimental results. *Tōhoku Geophys.*  
631 *Journ.*, 36, 452-455, 2003.
- 632 Bruhwiler, L., Dlugokencky, E., Masarie, K., Ishizawa, M., Andrews, A., Miller, J.,  
633 Sweeney, C., Tans, P., Worthy, D.: CarbonTracker-CH<sub>4</sub>: an assimilation system for  
634 estimating emissions of atmospheric methane, *Atmos. Chem. Phys.*, 14, 8269-8293,  
635 2014.
- 636 Bubier, J. L., Crill, P. M., Varner, R. K., and Moore, T. R.: BOREAS TGB-01/TGB-03  
637 CH<sub>4</sub> chamber flux data: NSA Fen. Data set, available at: <http://www.daac.ornl.gov>,  
638 Oak Ridge, TN, USA, 1998.
- 639 Chan, K. M., Wood, R.: The seasonal cycle of planetary boundary layer depth determined  
640 using COSMIC radio occultation data, *J. Geophys. Res.-Atmos.*, 118, 12,422-12,434,  
641 doi:10.1002/2013JD020147, 2013.
- 642 Chang, R. Y. W, Miller, C. E., Dinardo, S. J., Karion, A., Sweeney, C., Daube, B.,  
643 Henderson, J. M., Mountain, M. E., Eluszkiewicz, J., Miller, J. B., Bruhwiler, L. M. P.,  
644 Wofsy, S. C.: Methane emissions from Alaska in 2012 from CARVE airborne  
645 observations. *Proc. Natl. Acad. Sci.*, 111, 16694-16699, 2014.
- 646 Chapin, F. S.: Morphological and physiological mechanisms of temperature  
647 compensation in phosphate absorption along a latitudinal gradient, *Ecology*, 55, 1180-  
648 1198, 1974.
- 649 Clein, J. S., Schimel, J. P.: Microbial activity of tundra and taiga soils at sub-zero  
650 temperatures. *Soil. Biol. Biochem.*, 29(9), 1231-1234, 1995.
- 651 Clement, R. J., Verma, S. B., and Verry, E. S.: Relating Chamber Measurements to Eddy-  
652 Correlation Measurements of Methane Flux, *J. Geophys. Res.-Atmos.*, 100, 21047–  
653 21056, 1995.
- 654 Comas, X., Slater, L., Reeve, A.: Seasonal geophysical monitoring of biogenic gases in a  
655 northern peatland: implications for temporal and spatial variability in free phase gas

656 production rates, *J. Geophys. Res. Biogeosci.* 113, G01012,  
657 doi:10.1029/2007JG000575, 2008.

658 Ding, W. X., Cai, Z. C., and Wang, D. X.: Preliminary budget of methane emissions from  
659 natural wetlands in China, *Atmos. Environ.*, 38, 751–759,  
660 doi:10.1016/J.Atmosenv.2003.10.016, 2004.

661 Dise, N. B.: Methane Emission from Minnesota Peatlands-Spatial and Seasonal  
662 Variability, *Global Biogeochem. Cy.*, 7, 123–142, 1993.

663 Dunfield P, Knowles R, Dumont R, Moore TR. Methane production and consumption in  
664 temperate and subarctic peat soils: Response to temperature and pH. *Soil Biol*  
665 *Biochem* 1993; 25: 321–326.

666 Euskirchen, E. S., Bret-Harte, M. S., Scott, G. J., Edgar, C., Shaver, G. R.: Seasonal  
667 patterns of carbon dioxide and water fluxes in three representative tundra ecosystems  
668 in northern Alaska, *Ecosphere*, 1-19, 2012.

669 Granberg, G., Ottosson-Lofvenius, M., Grip, H., Sundh, I., and Nilsson, M.: Effect of  
670 climatic variability from 1980 to 1997 on simulated methane emission from a boreal  
671 mixed mire in northern Sweden, *Global Biogeochem. Cycles*, 15, 977–991, 2001.

672 Harazono, Y., Mano, M., Miyata, A., Yoshimoto, M., Zulueta, R. C., Vourlitis, G.L.,  
673 Kwon, H., Oechel, W.: Temporal and spatial differences of methane flux at arctic  
674 tundra in Alaska, *Natl Inst. Polar Res, Spec. Issue*, 59:79–95, 2006.

675 Hargreaves, K. J., Fowler, D., Pitcairn, C. E. R. and Aurela, M.: Annual methane  
676 emission from Finnish mires estimated from eddy covariance campaign  
677 measurements, *Theor. Appl. Climatol.* 70, 203–213, 2001.

678 Henderson, J. M., Eluszkiewicz, J., Mountain, M. E., Nehr Korn, T., Chang, R. Y.-W.,  
679 Karion, A., Miller, J. B., Sweeney, C., Steiner, N., Wofsy, S. C., Miller, C. E.,  
680 Atmospheric transport simulations in support of the Carve in Arctic Reservoirs  
681 Vulnerability Experiment (CARVE), *Atmos. Chem. Phys.*, 15,4093-4116, 2015.

682 Hinzman, L.D., L. A. Viereck, P. Adams, V. E. Romanovsky, and K. Yoshikawa, 2006.  
683 Climate and permafrost dynamics of the Alaskan boreal forest. In *Alaska's changing*  
684 *boreal forest*. Edited by F.S. Chapin III, M.W. Oswood, K Van Cleve, L.A. Viereck,  
685 and D.L. Verbyla. Oxford University Press, New York. pp. 39-61.

686 Hommeltenberg, J., Mauder, M., Drösler, M., Heidbach, K., Werle, P., Schmid, H. P.:  
687 Ecosystem scale methane fluxes in a natural temperature bog-pine forest in southern  
688 Germany, *Biogeosciences*, 11, 3477-3493, 2014.

689 Hugelius, G., Strauss, J., Zubrzycki, S., Harden, J. W., Schuur, E. A. G., Ping, C.-L.,  
690 Schirmermeister, L., Grosse, G., Michaelson, G. J., Koven, C. D., O'Donnell, J. A.,  
691 Elberling, B., Mishra, U., Camill, P., Yu, Z., Palmtag, J., Kuhry, P.: Estimated stocks  
692 of circumpolar permafrost carbon with quantified uncertainty ranges and identified  
693 data gaps, *Biogeosciences*, 11, 6573-6593, 2014.

694 IPCC: *Climate Change 2007: The Physical Science Basis. Contribution of Working*  
695 *Group I to the Fourth Assessment Report of the IPCC*, edited by: Solomon, S., Qin, D.,  
696 Manning, M., Chen, Z., Marquis, M., Averyt, K. B., Tignor, M., and Miller, H. L.,  
697 Cambridge University Press, Cambridge, United Kingdom and New York, 2007.

698 Iversen, C. M., Sloan, V. L., Sullivan, P. F., Euskirchen, E. S., McGuire, A. D., Norby, R.  
699 J., Walker, A. P., Warren, J. M., Wullschleger, S. D.:The unseen iceberg: plant roots  
700 in arctic tundra, *New Phytologist*, 205, 34-59, doi: 10.1111/nph.13003, 2015.

701 Iwata, H., Harazono, Y., Ueyama, M., Sakabe, A., Nagano, H., Kosugi, Y., Takahashi, K.,



702 Kim, Y.: Methane exchange in a poorly-drained black spruce forest over permafrost  
703 observed using the eddy covariance technique, *Agric. For. Meteorol.*, 214-215, 157-  
704 168 2015.

705 Jackowicz-Korczyński, M., Christensen, T. R., Bäckstrand, K., Crill, P., Friborg, T.,  
706 Mastepanov, M., Ström, L.: Annual cycle of methane emission from a subarctic  
707 peatland, *J. Geophys. Res.*, 115, G02009, doi:10.1029/2008JG000913, 2010.

708 Juutinen, S., Alm, J., Larmola, T., Huttunen, J. T., Morero, M., Martikainen, P. J.,  
709 Silvola, J.: Major implication of the littoral zone for methane release from boreal  
710 lakes, *Global Biogeochem. Cycles*, 17, 1117.10.1029/2003GB002105, 2003.

711 Karl, D. M., Tilbrook, B. D.: Production and transport of methane in oceanic particulate  
712 organic matter, *Nature*, 368, 732-734, 1994.

713 Keller, M. M.: Biological sources and sinks of methane in tropical habitats and tropical  
714 atmospheric chemistry, Princeton University, 1990.

715 King, J. Y., William, S. R., Shannon K. R.: Methane emission and transport by arctic  
716 sedges in Alaska: results of a vegetation removal experiment, *J. Geophys. Res.*, 103,  
717 29083-29092.

718 Kirschke, S., Bousquet, P., Ciais, P., Saunois, M., Canadell, J. G., Dlugokencky, E. J.,  
719 Bergamaschi, P., Bergmann, D., Blake, D. R., Bruhwiler, L., Cameron Smith, P.,  
720 Castaldi, S., Chevallier, F., Feng, L., Fraser, A., Heimann, M., Hodson, E. L.,  
721 Houweling, S., Josse, B., Fraser, P. J., Krummel, P. B., Lamarque, J., Langenfelds, R.  
722 L., Le Quéré, C., Naik, V., O'Doherty, S., Palmer, P. I., Pison, I., Plummer, D.,  
723 Poulter, B., Prinn, R. G., Rigby, M., Ringeval, B., Santini, M., Schmidt, M., Shindell,  
724 D. T., Simpson, I. J., Spahni, R., Steele, L. P., Strode, S. A., Sudo, K., Szopa, S., van  
725 der Werf, G. R., Voulgarakis, A., van Weele, M., Weiss, R. F., Williams, J. E., and  
726 Zeng, G.: Three decades of global methane sources and sinks, *Nat. Geosci.*, 6, 813–  
727 823, doi: 10.1038/ngeo1955, 2013.

728 Koh, H. S., Ochs, C. A., and Yu, K. W.: Hydrologic gradient and vegetation controls on  
729 CH<sub>4</sub> and CO<sub>2</sub> fluxes in a spring-fed forested wetland, *Hydrobiologia*, 630, 271–286,  
730 doi:10.1007/S10750-009-9821-X, 2009.

731 Koven, C. D., Riley, W. J., Subin, Z. M., Tang, J. Y., Torn, M. S., Collins, W. D., Bonan,  
732 G. B., Lawrence, D. M., Swenson, S. C.: The effects of vertically resolved soil  
733 biogeochemistry and alternate soil C and N models on C dynamics of CLM4,  
734 *Biogeosciences*, 10, 7109-7131, 2013.

735 Kummerow, J., Russell, M.: Seasonal root growth in the Arctic tussock tundra, *Oecologia*,  
736 47: 196–199, 1980.

737 Lupascu, M., Wadham, J. L., Hornibrook, E. R. C., Pancost, R. D.: Temperature  
738 sensitivity of methane production in the permafrost active layer at Stordalen, Sweden:  
739 A comparison with non-permafrost northern wetlands, *Arct., Antarc., Alp. Res.*, 44(4),  
740 469-482, 2012.

741 Mastepanov, M., Sigsgaard, C., Tagesson, T., Ström, L., Tamstorf, M. P., Lund, M.,  
742 Christensen, T. R.: Revisiting factors controlling methane emissions from high-arctic  
743 tundra, *Biogeosciences*, 10, 5139-5158, 2013.

744 Mastepanov, M., Sigsgaard, C., Dlugokencky, E. J., Houweling, S., Ström L., Tamstorf,  
745 M. P., and Christensen, T. R.: Large tundra methane burst during onset of freezing,  
746 *Nature*, 456, 628–631, 2008.

747 Mao, J., Shi, X., Thornton, P. E., Hoffman, F. M., Zhu, Z., Myneni, R. B., Global  
748 latitudinal-asymmetric vegetation growth trends and their driving mechanisms:2982-  
749 2009, *Remote Sens.*, 5 1484-1497, 2013.

750 McEwing, K. R., Fisher, J. P., Zona, D.: Environmental and vegetation controls on the  
751 spatial variability of CH<sub>4</sub> emission from wet-sedge and tussock tundra ecosystem in  
752 the Arctic, *Plant Soil*, 388, 37-52, 2015.

753 Melton, J. R., Wania, R., Hodson, E. L., Poulter, B., Ringeval, B., Spahni, R., Bohn, T.,  
754 Avis, C. A., Beerling, D. J., Eliseev, A. V., Denisov, S. N., Hopcroft, P. O.,  
755 Lettenmaier, D. P., Riley, W. J., Singarayer, J. S., Subin, Z. M., Tian, H., Zürcher,  
756 Brovkin, V., van Bodegom, P. M., Kleinen, T., Yu, Z. C., Kaplan, J. O., Present state  
757 of global wetland extent and wetland methane modeling: conclusions from a model  
758 inter-comparison project (WETCHIMP), *Biogeosciences*, 10, 753–788,2013.

759 Meng, L., Hess, P. G. M., Mahowald, N. M., Yavitt, J. B., Riley, W. J., Subin, Z. M.,  
760 Lawrence, D. M., Swenson, S. C., Jauhiainen, J., and Fuka, D. R.: Sensitivity of  
761 wetland methane emissions to model assumptions: application and model testing  
762 against site observations, *Biogeosciences*, 9, 2793–2819, doi:10.5194/bg-9-2793-  
763 2012, 2012.

764 Mialon, A., Royer, A., Fily, M.: Wetland seasonal dynamics and interannual variability  
765 over northern high latitudes, derived from microwave satellite data, *J. Geophys. Res.*,  
766 110, D17102, doi:10.1029/2004JD005697, 2005.

767 Moosavi, S. C., Crill, P. M., Pullman, E. R., Funk, D. W., Peterson, K. M.: Controls on  
768 CH<sub>4</sub> flux from an Alaskan boreal wetland, *Global Biogeochem. Cycles*, 10, 287-296,  
769 1996.

770 Morin, T. H., Bohrer, G., Naor-Azrieli, L., Mesi, S., Kenny, W. T., Mitsch, W. J.,  
771 Schäfer, K. V. R.: The seasonal and diurnal dynamics of methane flux at a created  
772 urban wetland. *Ecol. Engin.*, 72, 74-83, 2014.

773 Nakano, T., Kuniyoshi, S., Fukuda, M.: Temporal variation in methane emission from  
774 tundra wetlands in a permafrost area, northeastern Siberia. *Atmos. Environ.*, 34, 1205–  
775 1213, 2000.

776 Olivas, P. C., Oberbauer, S. F., Tweedie, C., Oechel, W. C., Lin, D., Kuchy, A.: Effects  
777 of Fine-Scale Topography on CO<sub>2</sub> Flux Components of Alaskan Coastal Plain Tundra:  
778 Response to Contracting Growing Seasons, *Arct. Antarct. Alpine Res.*, 43, 256–266,  
779 doi: 10.1657/1938-4246-43.2.256, 2011.

780 Peters, W., Jacobson, A. R., Sweeney, C., Andrews, A. E., Conway, T. J., Masarie, K.,  
781 Miller, J. B., Bruhwiler, L. M. P., Petron, G., Hirsch, A., Worthy, D. E. J., van der  
782 Werf G. R., Randerson, J. T., Wennberg, P. O., Krol, M. C., Tans, P. P.: An  
783 Atmospheric perspective on north American carbon dioxide exchange:  
784 CarbonTracker, *PNAS*, 18925-18930, 2007.

785 Pickett-Heaps, C. A., Jacob, D. J., Wecht, K. J., Kort, E. A., Wofsy, S. C., Diskin, G. S.,  
786 Worthy, D. E. J., Kaplan, J. O., Drevet, J.: Magnitude and seasonality of wetland  
787 methane emissions from the Hudson Bay Lowlands (Canada), *Atmos. Chem. Phys.*,  
788 11, 3773-3779, 2011.

789 Prigent, C., F. Papa, F. Aires, W. B. Rossow, E. Matthews.: Global inundation dynamics  
790 inferred from multiple satellite observations, 1993-2000, *J. Geophys. Res.-Atmos.*,  
791 112, D12107, doi:10.1029/2006JD007847, 2007.

792 Qian, T. T., Dai, A., Trenberth, K. E., and Oleson, K. W.: Simulation of global land

793 surface conditions from 1948 to 2004. Part I: Forcing data and evaluations, J.  
794 Hydrometeorol., 7, 953–975, 2006.

795 Riley, W. J., Subin, Z. M., Lawrence, D. M., Swenson, S. C., Torn, M. S., Meng, L.,  
796 Mahowald, N. M., Hess, P.: Barriers to predicting changes in global terrestrial  
797 methane fluxes: analyses using CLM4Me, a methane biogeochemistry model  
798 integrated in CESM, Biogeosciences, 8, 1025-1953, 2011.

799 Ringeval, B., de Noblet-Ducoudré, N., Ciais, P., Bousquet, P., Prigent, C., Papa, F.,  
800 Rossow, W. B.: An attempt to quantify the impact of changes in wetland extent on  
801 methane emissions on the seasonal and interannual time scales, Global Biogeochem.  
802 Cycles, 24, GB2003, doi:10.1029/2008GB003354, 2010.

803 Rinne, J., Riutta, T., Pihlatie, M., Aurela, M., Haapanala, S., Tuovinen, J., Tuittila, E.:  
804 Annual cycle of methane emission from a boreal fen measured by the eddy Covance  
805 technique., Tellus, 59B, 449-457, 2007.

806 Roulet, N. T., Ash, R., Moore, T.R.: Low boreal wetlands as a source of atmospheric  
807 methane, J. Geophys. Res., 97 (D4), 3739-3749, 1992.

808 Saarnio, S., Alm, J., Silvola, J., Lohila, A., Nykanen, H., and Martikainen, P. J.: Seasonal  
809 variation in CH<sub>4</sub> emissions and production and oxidation potentials at microsites on an  
810 oligotrophic pine fen, Oecologia, 110, 414–422, 1997.

811 Schroeder, R., McDonald K. C., Champan, B.D., Jensen, K., Podest, E., Tessler, Z. D.,  
812 Bohn, T. J., Zimmermann, R.: Development and evaluation of a multi-year fractional  
813 surface water data set derived from active/passive microwave remote sensing data, 7,  
814 16688-16732, 2015.

815 Schütz, H., Seiler, W., Conrad, R.: Influence of soil-temperature on methane emission  
816 from rice paddy fields, Biogeochemistry, 11, 77–95, 1990.

817 Segers, R.: Methane production and methane consumption: a review of process  
818 underlying wetland methane fluxes, Biogeochemistry, 41, 23-51, 1998.

819 Shannon, R. D. and White, J. R.: 3-Year Study of Controls on Methane Emissions from 2  
820 Michigan Peatlands, Biogeochemistry, 27, 35–60, 1994.

821 Siavoshi, M., Dastan, S., Yassari, E., Laware, S. L.: Role of organic fertilizers on  
822 morphological and yield parameters in rice ( *Oryza sativa* L.), Intl. J. Agron. Plant  
823 Prod., 4, 1220-1225, 2013.

824 Sloan, V.: Plant roots in Arctic ecosystems: stocks and dynamics and their coupling to  
825 aboveground parameters, *PhD Thesis. University of Sheffield*, Sheffield, UK, 2011.

826 Smith, L. K., Lewis, W. M., Chanton, J. P., Cronin, G., and Hamilton, S. K.: Methane  
827 emissions from the Orinoco River floodplain, Venezuela, Biogeochemistry, 51, 113–  
828 140, 2000.

829 Song, C., Xu, X., Sun, X., Tian, H., Sun, L., Miao, Y., Wang, X., Guo, Y.: Large  
830 methane emission upon spring thaw from natural wetlands in the northern permafrost  
831 region, Environ. Res. Lett., 7, 034009, doi:10.1088/1748-9326/7/3/034009, 2012.

832 Starr, G., Oberbauer, S., Ahlquist, L.: The photosynthetic response of Alaskan tundra  
833 plants to increased season length and soil warming, Arct. Antarct. Alp. Res. 40(1),  
834 181–191, 2008.

835 Sturtevant, C. S., Oechel, W. C., Zona, D., Kim, Y., and Emerson, C. E.: Soil moisture  
836 control over autumn season methane flux, arctic coastal plain of Alaska,  
837 Biogeosciences, 9, 1423–1440, 2012.

838 Sullivan, P. F., Welker, J. M.: Warming chambers stimulate early season growth of an  
839 arctic sedge: results of a minirhizotron field study, *Oecologia*, 142, 616-626, 2005.

840 Svensson, B. H., Christensen, T. R., Johansson, E., and Oquist, M.: Interdecadal changes  
841 in CO<sub>2</sub> and CH<sub>4</sub> fluxes of a subarctic mire: Stordalen revisited after 20 years, *Oikos*, 85,  
842 22–30, 1999.

843 Tian, Y., Dickinson, R. E., Zhou, L., Zeng, X., Dai, Y., Myneni, R. B., Knyazikhin, Y.,  
844 Zhang, X., Friedl, M., Yu, H., Wu, W., Shaikh, M.: Comparison of seasonal and  
845 spatial variations of leaf area index and fraction of absorbed photosynthetically active  
846 radiation from Moderate Resolution Imaging Spectroradiometer (MODIS) and  
847 Common Land Model, *J. Geophys. Res.*, 109, D01103, doi:10.1029/2003JD003777,  
848 2004.

849 Tokida, T., Mizoguchi, M., Miyazaki, T., Kagemoto, A., Nagata, O., Hatano, R.:  
850 Episodic release of methane bubbles from peatland during spring thaw, *Chemosphere*,  
851 70, 165-171, 2007.

852 Torn, M. S., and Chapin III, F. S.: Environmental and biotic controls over methane flux  
853 from arctic tundra, *Atmos. Environ.*, 32, 3201–3218, 1993.

854 van Fischer, J. C., Rhew, R. C., Ames, G. M., Fosdick, B. K., von Fischer, P. E.:  
855 Vegetation height and other controls of spatial variability in methane emissions from  
856 the Arctic coastal tundra at Barrow, Alaska, *J. Geophys. Res.*, 115, G00I03,  
857 doi:10.1029/2009JG001283, 2010

858 van Hulzen J.B., Segers, R., van Bodegom, P. M., Leffelaar, P.A.: Temperature effects on  
859 soil methane production: and explanation for observed variability, *Soil Biol. and*  
860 *Biochem.*, 31, 1919-1929, 1999.

861 van Winden, J. F., Reichart, G.-J., McNamara, N. P., Benthien, A., Damsté, J. S. S.:  
862 Temperature-induced increase in methane release from peat bogs: a mesocosm  
863 experiment, *PLoS ONE* 7(6): e39614. doi:10.1371/journal.pone.0039614, 2012.

864 Verma, A., Arkebauer, T. J., and Valentine, D.: BOREAS TF-11 CO<sub>2</sub> and CH<sub>4</sub> flux data  
865 from the SSA-Fen. Data set, available at: <http://www.daac.ornl.gov>, Oak Ridge, TN,  
866 USA, 1998.

867 Wang, C., Xiao, S., Li, Y., Zhong, H., Li, X., Peng, P.: Methane formation and  
868 consumption processes in Xiangxi Bay of the Three Gorges Reservoir, *Sci. Rep.* 4,  
869 444, doi:10.1038/srep04449, 2014.

870 Wania, R., Ross, I., and Prentice, I. C.: Implementation and evaluation of a new methane  
871 model within a dynamic global vegetation model: LPJ-WHyMe v1.3.1, *Geosci. Model*  
872 *Dev.*, 3, 565–584, doi:10.5194/gmd-3-565-2010, 2010.

873 Wassmann, R., Thein, U. G., Whiticar, M. J., Rennenberg, H., Seiler, W., and Junk, W. J.:  
874 Methane emissions from the Amazon floodplain: Characterization of production and  
875 transport, *Global Biogeochem. Cy.*, 6, 3–13, 1992.

876 Whalen, S. C., Reeburgh, W. S.: Consumption of atmospheric methane by tundra soils,  
877 *Nature*, 342, 160–162, 1990.

878 Whalen, S. C. and Reeburgh, W. S.: Interannual variations in tundra methane emission: a  
879 4-year time series at fixed sites., *Global Biogeochem. Cy.*, 6, 139–159, 1992.

880 Whiting, G. J., Chanton, J. P.: Greenhouse carbon balance of wetlands: Methane emission  
881 versus carbon sequestration, *Tellus*, 53B, 521-528, 2001.

882 Wickland, K. P., Striegl, R. G., Schmidt, S. K., Mast, M. A.: Methane flux in subalpine  
883 wetland and unsaturated soils in the southern Rocky Mountains, *Global Biogeochem.*  
884 *Cycles*, 13, 101–113, 1999.

885 Wilson, J. O., Crill, P. M., Bartlett, K. B., Sebacher, D. I., Harriss, R. C., Sass, R. L.:  
886 Seasonal variation of methane emissions from a temperate swamp, *Biogeochemistry*,  
887 8, 55-71, 1998.

888 Yvon-Durocher, G., Montoya, J. M., Woodward, G., Jones, J. I., Trimmer, M.: Warming  
889 increases the proportion of primary production emitted as methane from freshwater  
890 mesocosms, *Global Chang. Biol.*, 17, 1225-1234, 2011.

891 Yvon-Durocher, G., Allen, A. P., Bastviken, D., Conrad, R., Gudas, C., St-Pierre, A.,  
892 Thanh-Duc, N., del Giorgio, P. A.: Methane fluxes show consistent temperature  
893 dependence across microbial to ecosystem scale, *Nature*, 507, 488-491, 2014.

894 Zhuang, Q., Melillo, J. M., Kicklighter, D. W., Prinn, R. G., McGuire, A. D., Steudler, P.  
895 A., Felzer, B. S., and Hu, S.: Methane fluxes between terrestrial ecosystems and the  
896 atmosphere at northern high latitudes during the past century: A retrospective analysis  
897 with a process based biogeochemistry model, *Glob. Biogeochem. Cycles*, 18,  
898 GB3010, doi:3010.1029/2004GB002239, 2004.

899 Zona, D., Oechel, W. C., Kochendorfer, J., Paw U, Salyuk, A. N., Olivas, P. C.,  
900 Oberbauer, S. F., Lipson, D. A.: Methane fluxes during the initiation of a large-scale  
901 water table manipulation experiment in the Alaskan Arctic tundra, *Global*  
902 *Biogeochem. Cycle* 23, GB2013, doi:10.1029/2009GB003487, 2009.

903 Zona, D., Gioli, B., Commane, R., Lindaas, J., Wofsy, S. C., Miller, C. E., Dinardo, S. J.,  
904 Dengel, S., Sweeney, C., Karion, A., Chang, R.Y.-W., Henderson, J. M., Murphy, P.  
905 C., Goodrich, J. P., Moreaux, V., Liljedahl, A., Watts, J. D., Kimball, J. S., Lipson, D.  
906 A., Oechel, W. C.: Cold season emissions dominate the Arctic tundra methane budget,  
907 *PNAS*, 113,40-45, 2016.

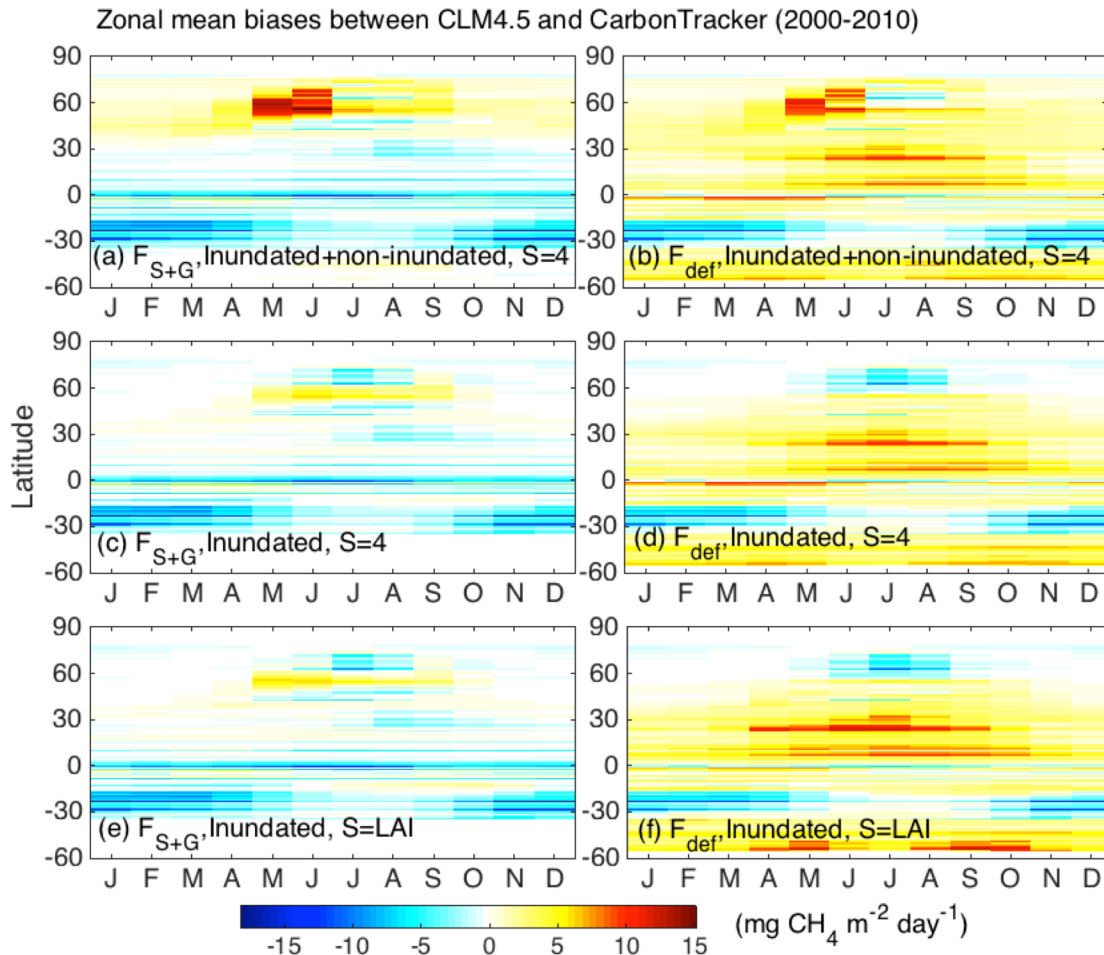


Fig. 1. Zonal mean biases of CH<sub>4</sub> emissions between CLM4.5 predictions and CarbonTracker (CH<sub>4</sub> CLM4.5-CH<sub>4</sub> CarbonTracker) with SWAMPS-GLWD ( $F_{S+G}$ ) and CLM4.5 predicted ( $F_{def}$ ) inundation fraction: CLM4.5 predictions of both inundated and noninundated emissions with  $F_{S+G}$  (a) and  $F_{def}$  (b), while aerechyma area is corrected with  $S=4$ ; CLM4.5 predictions of inundated emissions only with  $F_{S+G}$  (c) and  $F_{def}$  (d), while aerechyma area is corrected with  $S=4$ ; CLM4.5 predictions of inundated emissions only with  $F_{S+G}$  (e) and  $F_{def}$  (f), while aerechyma area is parameterized by default  $S=LAI$ .



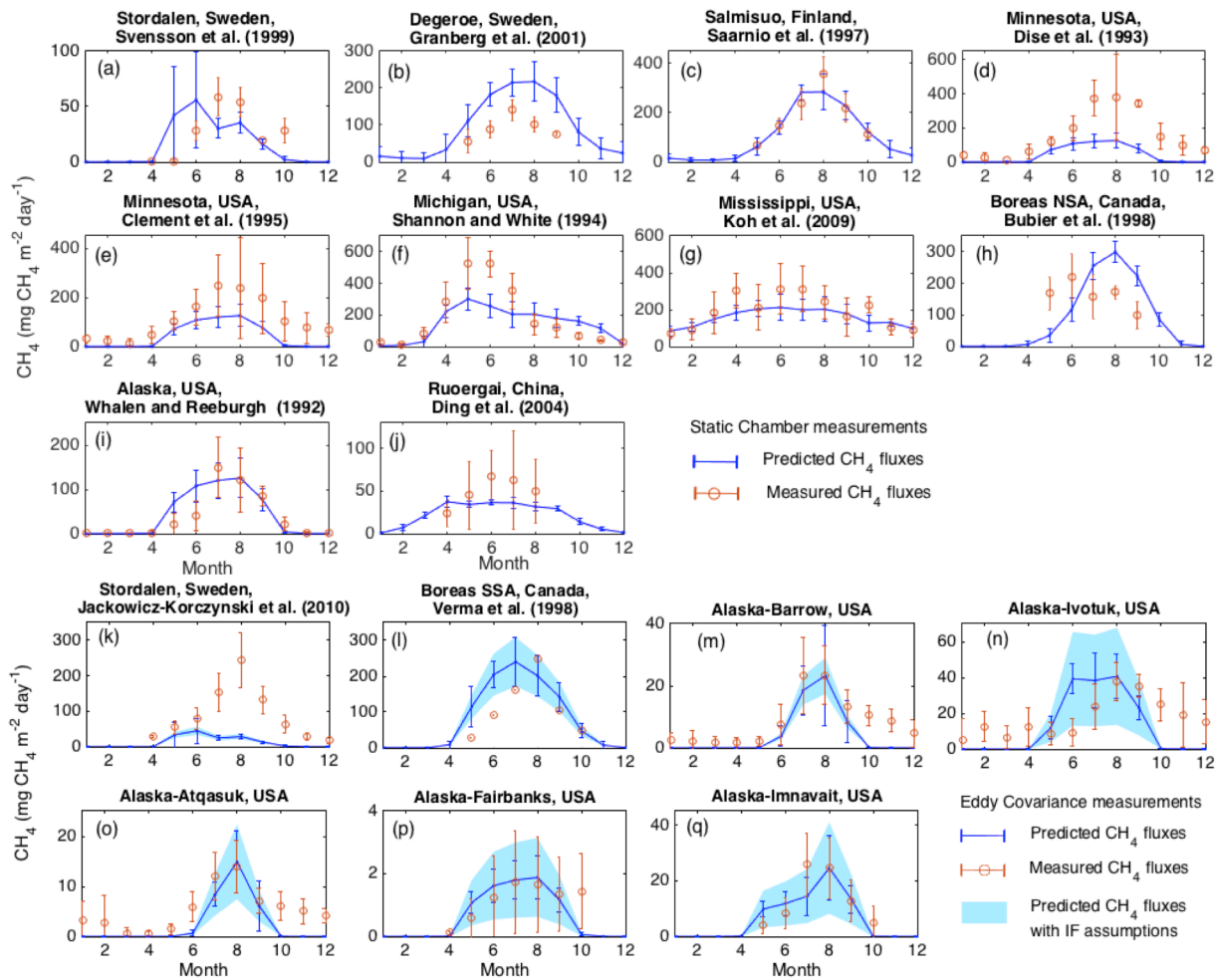


Fig. 2. Comparison of monthly mean simulated net CH<sub>4</sub> flux between 2000 and 2012 and observed monthly mean net CH<sub>4</sub> emissions in measurement year(s). The site measurements with static chamber are shown in (a-j) and measurements with eddy covariance (EC) towers are shown in (k-q). The error bars are standard deviation of monthly mean. The measurements with EC tower are weighted with a range of **Inundation Fraction (IF)** based on best estimates available: Stordalen: 80-100%; Boreas SSA: 50-90%; Alaska-Barrow: 60-100%, Alaska-Atqasuk: 10-30%; Alaska-Ivotuk: 5-25%; Alaska-Fairbanks: 0.5-2.5%, Alaska-IMN: 5-25%. Detailed description of the sites and measurements are shown in Table S1.

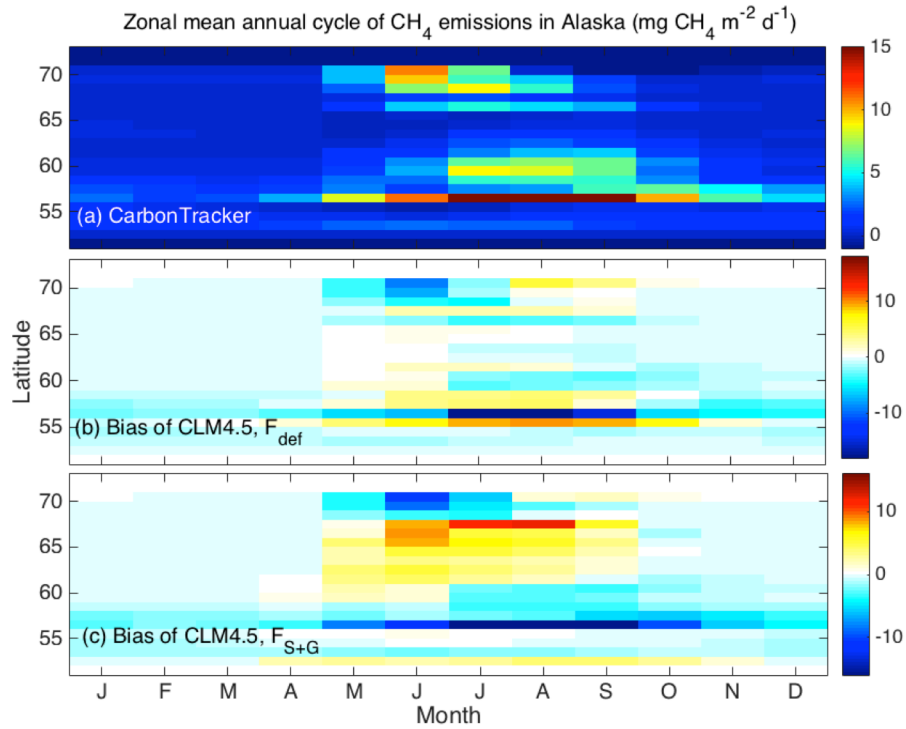


Fig. 3. The 2000-2010 zonal mean annual cycle of  $\text{CH}_4$  emission ( $\text{mg CH}_4 \text{ m}^{-2} \text{ day}^{-1}$ ) across Alaska predicted by CarbonTracker (a), and biases of CLM4.5 with CLM4.5 predicted inundation fraction ( $F_{def}$ ) (b) and SWAMPS-GLWD inundation fraction ( $F_{S+G}$ ) (c). The  $0.5^\circ \times 0.5^\circ$  CLM4.5 is regridded to  $1^\circ \times 1^\circ$  to be consistent with CarbonTracker.

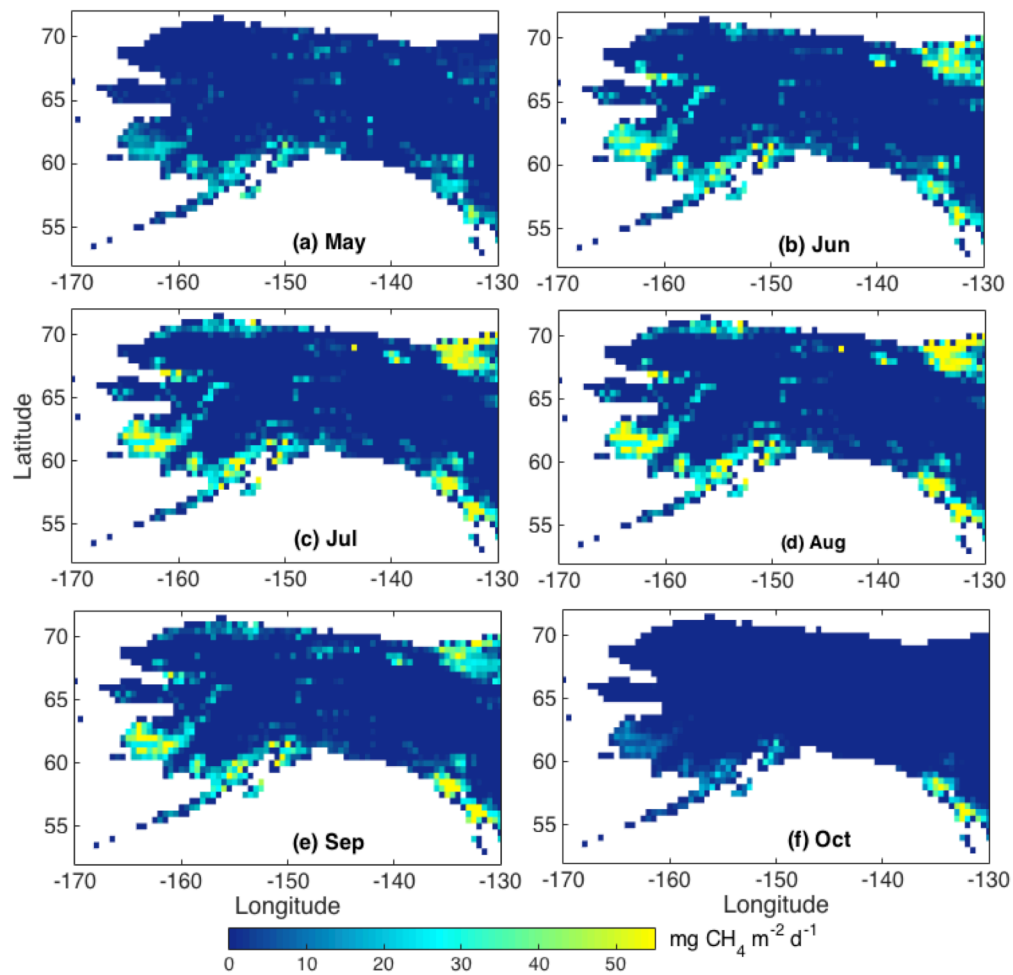


Fig. 4. CLM4.5 simulated mean monthly CH<sub>4</sub> emissions with  $F_{def}$  across years 2000-2012.

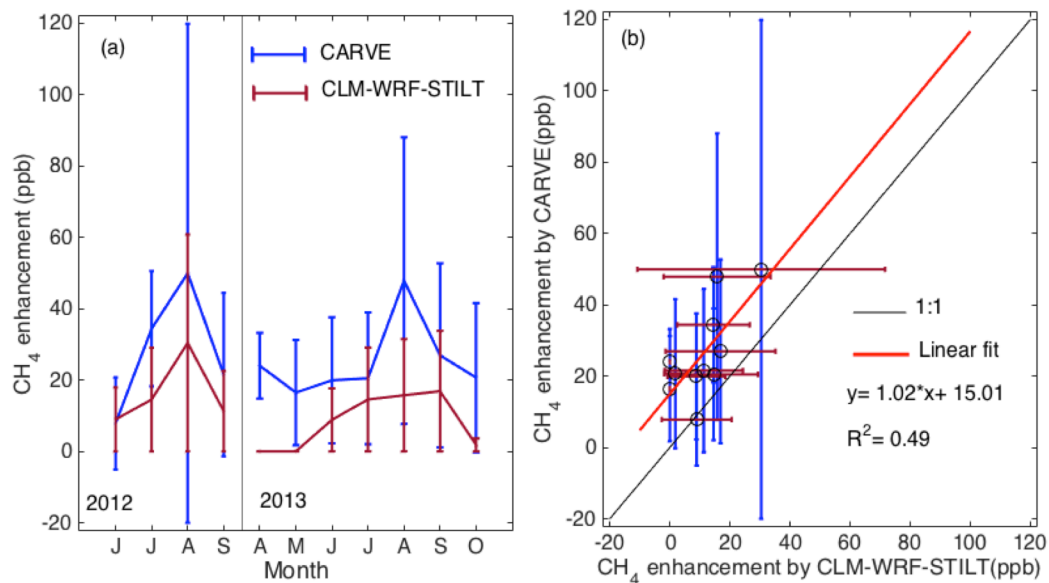


Fig. 5. The monthly mean atmospheric mole fraction enhancements in CH<sub>4</sub> estimated by WRF-STILT-CLM4.5 and CARVE measurements. (a) Observed and simulated monthly CH<sub>4</sub> mole fraction enhancements in 2012 and 2013; (b) Linear regression of measured versus modeled CH<sub>4</sub> mole fraction enhancements. The error bars are standard deviation of monthly mean.

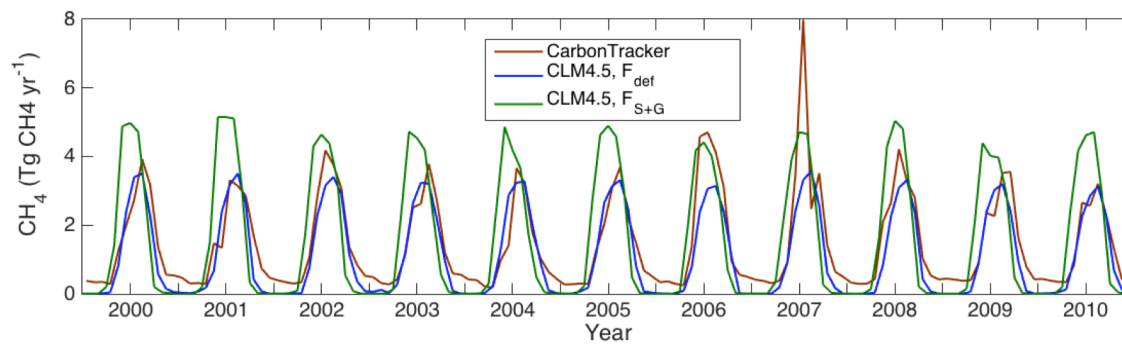


Fig. 6. Time variation of integrated CH<sub>4</sub> (Tg CH<sub>4</sub> yr<sup>-1</sup>) emissions from Alaska by CarbonTracker (brown), CLM4.5 with internally-predicted fraction of inundation  $F_{def}$  (blue) and CLM4.5 SWAMPS-GLWD fraction of inundation  $F_{S+G}$  (green).

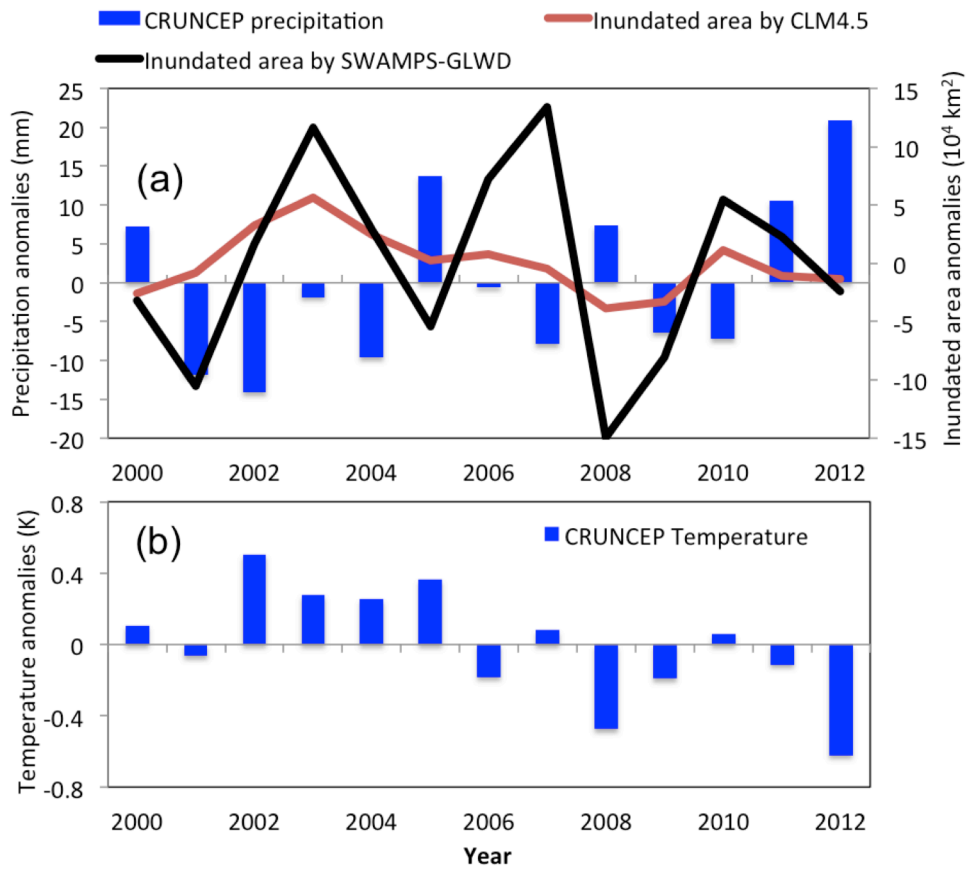


Fig. 7. The anomalies of annual precipitation and inundated area in Alaska (a) and the anomalies of annual mean temperature (b). The anomalies are calculated by subtracting the average between 2000-2012.

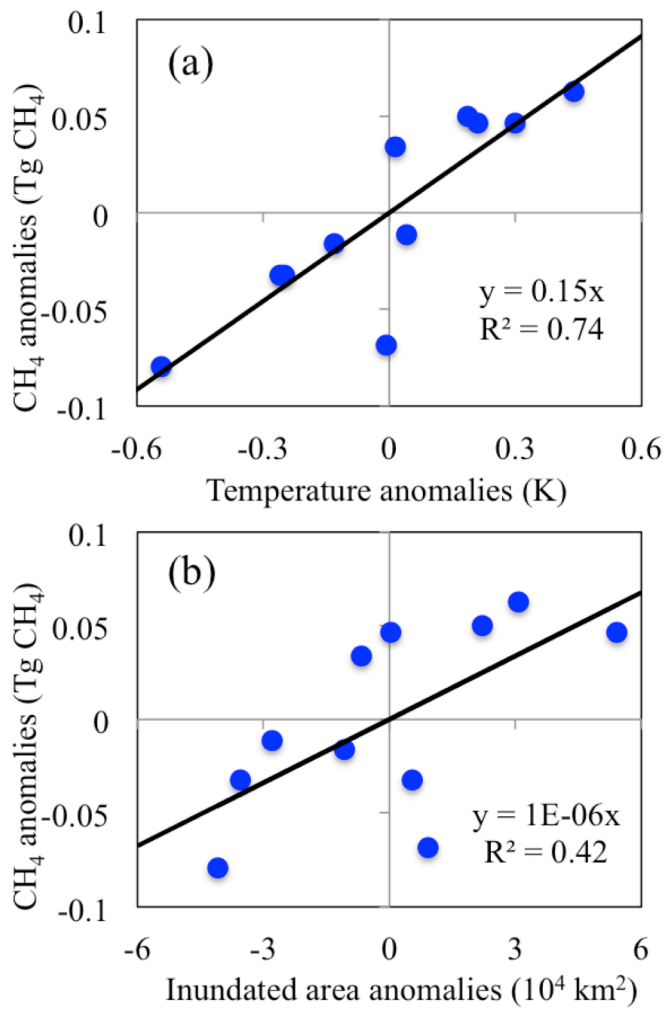


Fig. 8. The correlation between CLM-predicted annual CH<sub>4</sub> emission anomalies and mean annual temperature anomalies (a) and correlation between annual CH<sub>4</sub> emission anomalies and predicted inundated area anomalies during 2000-2010. The anomalies are calculated by subtracting the average between 2000-2010.



## Supplement

### A multi-scale comparison of modeled and observed seasonal methane emissions in northern wetlands

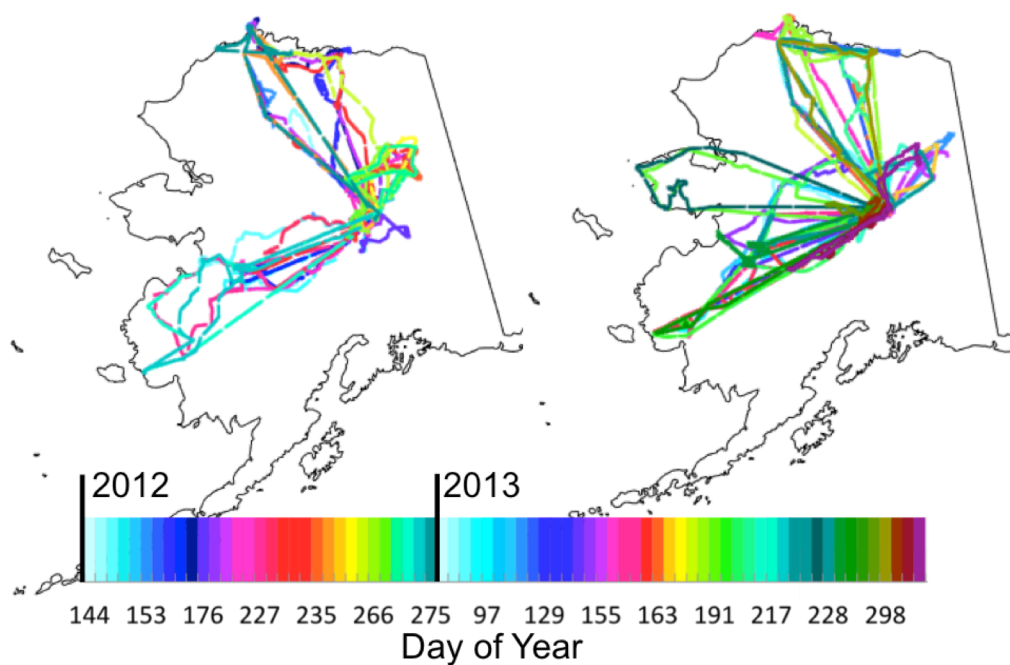


Fig. S1. Flight tracks with valid CH<sub>4</sub> mole fractions during the CARVE 2012 and 2013 campaigns. There were 31 flight days in 2012 and 43 flight days in 2013 (Supplement Table S2).

Site Name	Site Location (Lat, Lon)	Citation	Measurement Method	Data years
Ruoergai, China	32°47'N, 102°32'E	Ding et al. (2004)	SC	2001, 2002
Mississippi, USA	34°24'N, 89°50'W	Koh et al. (2009)	SC	2005, 2006
Michigan, USA	42°27'N, 84°01'W	Shannon and White (1994)	SC	1991, 1992, 1993
Minnesota, USA	47°32'N, 93°28'W	Clement et al. (1995)	SC	1991, 1992
Minnesota, USA	47°32'N, 93°28'W	Dise(1993)	SC	1988, 1989, 1990
Boreas NSA-Fen, Canada	55°55'N, 98°25'W	Bubier et al. (1998)	SC	1994, 1996
Salmisuo, Finland	62°47'N, 30°56'E	Saarnio et al.( 1997)	SC	1993
Degeröe, Sweden	64°11'N, 19°33'E	Granberg et al. (2001)	SC	1995, 1996, 1997
Alaska, USA	64°52'N, 147°51'W	Whalen and Reeburgh (1992)	SC	1987,1988, 1989, 1990
Stordalen, Sweden	68°20'N, 19°03E	Svensson et al. (1999)	SC	1974, 1994, 1995
Boreas SSA-Fen, Canada	53°48'N, 104°37'W	Verma et al.(1998)	EC	1994, 1995
Stordalen, Sweden	68°20'N, 19°03E	Jackowicz-Korczynski et al. (2010)	EC	2006, 2007
Alaska-BEO1, USA	71°17'N, 156°37'W	Raz-Yaseef, N. (NGEE-Arctic)	EC	2012, 2013
Alaska-BEO2, USA	71°17'N, 156°37'W	Zona et al., (2016)	EC	2013, 2014
Alaska-BES, USA	71°17'N, 156°36'W	Zona et al., (2016)	EC	2013, 2014
Alaska-CMDL, USA	71°19'N, 156°37'W	Zona et al., (2016)	EC	2013, 2014
Alaska-ATQ, USA	70°28'N, 157°25'W	Zona et al., (2016)	EC	2013, 2014
Alaska-IVO, USA	68°29'N, 155°45'W	Zona et al., (2016)	EC	2013, 2014
Alaska-FAI, USA	64°52'N, 147°51'W	Iwata et al., (2015)	EC	2011, 2012, 2013
Alaska-IMN, USA	68°37'N, 149°18'W	EUSKIRCHEN, E. S. (UAF)	EC	2012, 2013, 2014

Table S1. Summary of the sites and measurements used in comparison with model prediction. SC: static chamber; EC: eddy covariance tower.

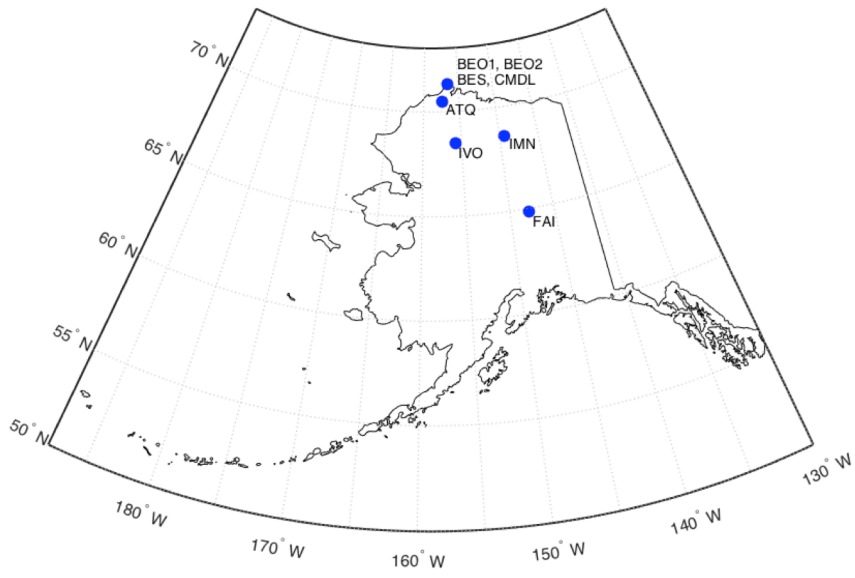


Fig. S2 The eight eddy covariance (EC) sites in Alaska

Table S2. The flight dates of CARVE measurements in 2012 and 2013

Year	Month	Dates
2012	May	23,24,27,28,30
	June	1,18,19,21,22,24
	July	17,22,24,25
	August	14,18,19,20,21,22,23
	September	17,18,19,21,22,23,24,26
	October	1
2013	April	2,3,4,5,6
	May	2,4,6,7,8,9,10,13
	June	2,3,6,7,8,9,11
	July	3,4,5,7,9,11,12
	August	2,3,4,7,11,12,13
	September	5,6,7,10,12
	October	24,25,26,27